UNIVERSITY OF CANTERBURY
Te Whare Wānanga o Waitaha
CHRISTCHURCH NEW ZEALAND

Recommended Revisions to the Approach in NZS 1170.5:2004 for the Seismic Design of Parts and Components

Provided to Toka Tū Ake | the New Zealand Earthquake Commission

Prepared by

Kieran Haymes

Professor Timothy John Sullivan

Te Tari Pūhanga Metarahi, Rawa Taiao | Department of Civil and Natural Resources Engineering

University of Canterbury

Revision 2

Christchurch, New Zealand

January 2023

Disclaimer

The contents of this work reflect the findings and recommendations of the authors, based on the research they have conducted and information obtained from the literature, as described within the report. Parts of the report have been prepared using external sources, systems and other information that is considered to be accurate, complete and reliable at the time of preparation, but the accuracy and completeness cannot be guaranteed. The authors make no representation or warranty, express or implied, as to the accuracy or completeness of the information contained within this Report, and nothing in this Report shall be deemed to constitute any representation or warranty. To the fullest extent permitted by law, the authors and the University of Canterbury shall not be liable or responsible for any error or omission in this Report.

.

Abstract

This report examines the current state of practice for the design for seismic loading of parts and components within buildings in New Zealand and the provisions recently developed by the Applied Technology Council subsequently adopted in ASCE 7-22. The findings of the research suggest that revisions should be made to *Section 8 Requirements for Parts and Components* of the New Zealand Standard *NZS 1170.5:2004 Structural Design Actions, Part 5: Earthquake Actions*. Updates to the parts and components approach are recommended, benefitting from insight provided through the recent ASCE 7-22 procedure and research in the literature. To gauge the performance of the parts and components approach with updates, comparisons are made with data from instrumented buildings and numerical models.

TABLE OF CONTENTS

1 Introduction 1
1.1 Context of Seismic Demands on Parts and Components 1
1.2 Approaches for the Prediction of Seismic Demands on Parts and Components 2
1.2.1 Time-history analysis 2
1.2.2 Modal superposition approaches 2
1.2.3 Code approaches 3
1.3 Objectives of this Study and Layout of this Report 3
2 Data Used to Evaulate Approaches 5
2.1 Instrumented Buildings 5
2.2 Numerical Analyses 6
3 The Current New Zealand Design Standard Approach 7
3.1 General Equation for the Horizontal Design Actions on Parts and Components 7
3.2 Floor Height Coefficient 8
3.3 Part Spectral Shape Factor 12
3.4 Part Response Factor 14
4 The ASCE/SEI 7-22 Approach 16
4.1 General Equation for the Horizontal Design Actions on Parts and Components 16
4.2 Floor Height Amplification Factor 17
4.3 Structure Ductility Factor 20
4.4 Component Resonance Ductility Factor 22
4.5 Component Strength Factor 22
4.6 Upper and Lower Bounds 23
4.6.1 Upper Bound 23
4.6.2 Lower Bound 23
5 June 2022 Workshop with Engineering Practitioners and Academics to Review Parts and Components Provisions in New Zealand 25
5.1 Overview of the Workshop 25
5.2 Outcomes from the Workshop 26
6 Recommended Revisions to the New Zealand Design Standard 28

6.1 General Equation for the Horizontal Design Actions on Parts and Components 28
6.2 Ground Motion Intensity 29
6.3 Floor Height Coefficient 30
6.4 Structural Nonlinearity Reduction Factor 31
6.5 Part or Component Spectral Shape Coefficient 35
6.5.1 Defining Rigid and Flexible Parts and Components 35
6.5.2 Maximum Dynamic Amplification 36
6.6 Part or Component Response Factor 38
6.7 Upper Bound of the Horizontal Design Force 39
6.8 Long Period Parts and Components 40
6.9 Torsional Structural Response and In-Plane Diaphragm Flexibility 44
7 Comparison of Design Loads Estimated using the Recommended and Current Approaches 46
8 Conclusions 64
9 References 66

1 INTRODUCTION

1.1 Context of Seismic Demands on Parts and Components

Secondary structural and non-structural parts, elements, or components, comprise between approximately eighty to ninety percent of construction cost of new buildings (Khakurel *et al.*, 2020). As a consequence, earthquakes can cause significant financial losses due to damage to parts and components, which may be compounded by disruption and downtime (Filiatrault & Sullivan, 2014). Significant damage to parts and components was observed following the 2010 and 2011 Canterbury earthquake sequence which, at times, attracted scrutiny over the future of otherwise repairable structures (Dhakal *et al.*, 2016; Khakurel *et al.*, 2020). More recently, the 2013 and 2016 earthquakes centred in the upper South Island resulted in damage to parts and components in Wellington (Chandramohan *et al.*, 2017). Whilst most damage to parts and components causes loss and disruption, the failure of parts and components can pose a life-safety hazard either by falling heavy objects (Villaverde, 1997) or by disrupting egress routes.

Parts and components may provide functionality, including mechanical plant, electrical services, and plumbing; form architectural features, such as ceilings, glazing, partition walls, and ornamentation; or as contents, like furniture, fixings, and other equipment (FEMA, 2012). Parts and components are often classified by engineers though definition of the type of demands that can induce damage during earthquake motions. This is generally denoted as sensitivity to acceleration, inter-storey drift, or a combination of both actions. The control of drift demands imposed on non-structural components is often addressed during the design of the primary structure. The seismic design of acceleration-sensitive non-structural components, however, requires further analysis to determine the demands that are imposed (Calvi & Ruggiero, 2017; Rashid *et al.*, 2021; Sullivan *et al.*, 2013).

The seismic response of acceleration-sensitive parts or components is defined by a series of physical behaviours and interactions, as illustrated in Figure 1.1. The earthquake shaking at the base of a building will be influenced by local seismology and site conditions, which affects the intensity and duration of ground motions. The building characteristics of mass, stiffness, damping and strength will then dictate the motion of the floors that parts or components are supported from. The response of the components to this motion will then vary according to the characteristics of the part of component, including its bracing and attachments. The peak demands imposed upon parts or components will therefore be influenced by many parameters and their associated uncertainties.

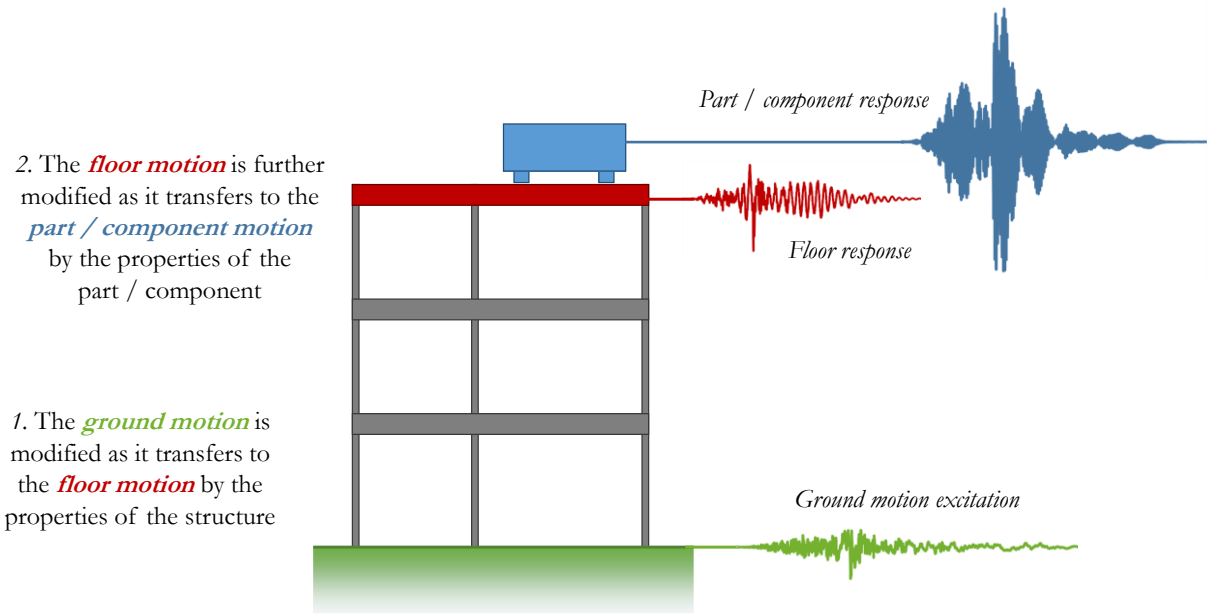

Figure 1.1: The response of parts or components depends on ground motion excitation at the base of the structure, as well as the properties of the structure and the parts or components.

1.2 Approaches for the Prediction of Seismic Demands on Parts and Components

Seismic demands on parts and components may be estimated using methods of varying complexity, specificity, and accuracy. The balance between computational efficiency and reliability is the fundamental issue for the development of a method that can be adopted in engineering practice, where the resources that may be allocated to the seismic design of parts and components can be limited.

1.2.1 Time-history analysis

Parts and components, and the structure that supports them, may be explicitly modelled using time history analysis. Highly accurate predictions may be achieved if sufficient information about the structural system and the part and component is available and appropriately modelled owing to the high degree of specificity this approach requires. However, if poor modelling assumptions are made, predictions from time history analysis can be very inaccurate. As this approach requires significant computational resources and the significant knowledge of the building structure, the applicability of this approach in engineering practice is limited.

1.2.2 Modal superposition approaches

There are some promising contemporary methods for prescribing floor acceleration response spectra developed by Sullivan *et al.* (2013), Vukobratović and Fajfar (2017), and Welch and Sullivan (2017), as well as methods for floor displacement response spectra by Calvi (2014) and Merino *et al.* (2020), or both by Haymes (2022). These methods use the superposition of modal contributions and establish empirical factors to account for many influential parameters.

ASCE/SEI 7-16 (American Society of Civil Engineers, 2017) permitted the use of a simplified modal superposition method using a floor acceleration response spectrum constructed considering amplifications due to structural modes, derived from work by Kehoe and Hachem (2003). The simplifications adopted in this approach have been shown to result in poorer predictions than other modal superposition approaches when compared to floor response spectra computed from instrumented building data (Haymes *et al.*, 2020), despite requiring a similar amount of knowledge of parameters. This approach was subsequently removed in the current ASCE/SEI 7-22 (American Society of Civil Engineers, 2021).

Although modal superposition approaches appear to offer a rigorous and reliable, yet reasonably simple, prediction method for adoption in industry, a workshop has been conducted with New Zealand engineering practitioners to gauge their views on such approaches for possible inclusion in design standards and is reported later in Section 5.

1.2.3 Code approaches

Code approaches utilise simplified expressions to relate ground shaking intensity to acceleration demands and strength requirements for parts and components. The resources and time that can be provided to the design of parts and components in engineering practice are often limited by economic considerations. The design procedures used by engineering practitioners must therefore balance the requirement for reliable estimation with the simplicity and speed of use. Further, the parameters required for the application of design approaches may be constrained by the information on the building and the part or component that is accessible to the practitioner or technician who is conducting the design. Accordingly, the design standards that are implemented in design practice internationally tend to favour simplicity and ease of application over specificity and complexity, and consequently require several assumptions on the dynamics that influence the seismic demands on parts and components.

In New Zealand, the legal requirements for buildings are specified in the Building Code may be achieved using design standards that are deemed to be a means of compliance. The seismic design of parts and components addresses the requirements of B1 Structure and is often conducted using Section 8 Requirements for Parts and Components of the New Zealand Standard NZS 1170.5:2004 Structural Design Actions, Part 5: Earthquake Actions (Standards New Zealand, 2016a). The details of the provisions for the part horizontal design force, the focus of this study, are reviewed in Section 3 of this report.

1.3 Objectives of this Study and Layout of this Report

This report details recommendations to update the method to determine the seismic demands on parts and components in buildings used by New Zealand design practitioners. The recommended approach outlined in this report attempts to address this desire, to enable the adoption of a practice-oriented method that has a strong rational basis.

The data used throughout the study to verify and examine the performance and assumptions of the current and recommended design provisions are described first in Section 2. The current design provisions in NZS1170.5 are then outlined and examined, followed by those proposed by the ATC-120 report and subsequently adopted in ASCE 7-22, in Sections 3 and 4, respectively. The workshop with New Zealand engineering practitioners and academics is then discussed in Section 5, with key findings examined. The recommended approach is then outlined and verified in Section 6, and applied to case study design examples in Section 7. From this, several conclusions are drawn to support the consideration of the recommended approach for future adoption into engineering practice within New Zealand.

2 DATA USED TO EVAULATE APPROACHES

2.1 Instrumented Buildings

The seismic demands on parts and components within elastically responding structures is examined here considering floor motions from recent earthquakes recorded under the GeoNet Structural Array instrumented building programme (GeoNet, 2022). The structures examined in this work comprise the two seismically-separated Avalon GNS buildings (Units One and Two), the University of Canterbury Physics (UC Physics) building, the Ministry of Business, Innovation, and Employment (MBIE) Stout St building, Wellington Hospital, the Nelson Marlborough Institute of Technology (NMIT) building, the Victoria University Te Puni Village building, the Majestic Centre, and the Bank of New Zealand (BNZ) CentrePort building. A summary of the properties of these buildings is provided in Table 2.1. In each building, the longitudinal and transverse responses were recorded at each instrumented floor by triaxial accelerometers.

At the UC Physics building motions from the 2010/2011 Canterbury earthquake sequence (M4.7 to M6.3) were recorded, where minor cracking of the concrete structure was observed (McHattie, 2013). Motions were recorded in the 2013 Seddon (M6.5) and Grassmere (M6.6) earthquakes by the GNS, Wellington Hospital, NMIT, Victoria University, and Majestic Centre buildings. The 2016 M7.8 Kaikōura earthquake motions were recorded at the GNS, Wellington Hospital, NMIT, and MBIE buildings. All buildings are assumed to have remained within the elastic range, with the exception of the BNZ CentrePort building, which developed significant inelasticity (Chandramohan et al., 2017) resulting in its demolition.

Table 2.1: Overview of GeoNet instrumented buildings used as case studies.

Building	Location	No. of Storeys	Lateral load resisting system	Year built	Year instr.ed	Instruments available
University of Canterbury Physics Building	Christchurch	8	Coupled reinforced concrete shear walls	1961	2007	10
Avalon GNS Unit 1	Lower Hutt	3	Reinforced concrete moment frame	1973	2007	4
Avalon GNS Unit 2	Lower Hutt	3	Reinforced concrete moment frame	1973	2007	5
MBIE Stout St	Wellington	9	Concrete-encased steel moment frame	1940	2014	16
Wellington Hospital	Wellington	6	Base-isolated reinforced concrete moment frame	2008	2009	16
Nelson Marlborough Institute of Technology	Nelson	3	Timber shear walls with energy dissipating devices	2011	2011	9
Victoria University Te Puni Village	Wellington	10	Rocking steel moment frame	2009	2009	12
Majestic Centre	Wellington	28	Reinforced concrete shear walls	1990	2011	15
BNZ CentrePort	Wellington	5	Reinforced concrete moment frame	2009	2009	16

2.2 Numerical Analyses

The seismic demands on parts and components within inelastically responding structures is examined here using results from time history analyses conducted by Welch and Sullivan (2017). That study examines the response of steel moment resisting frame (referred to as stiff steel MRFs by Welch and Sullivan (2017)) and reinforced concrete wall lateral load resisting systems, using four-, eight-, and twelve-storey structures. The forty-four recorded ground motions comprising the FEMA P695 far-field set (Federal Emergency Management Agency, 2009) were used to impose earthquake actions. The ground motions were scaled to six intensity levels using scale factors producing median peak ground accelerations from 0.15 g to 0.9 g. The steel MRF buildings were also run at a seventh intensity level of 1.2 g. The analyses were conducted using RUAUMOKO3D (Carr, 2006) with two-dimensional centreline models. An effective system displacement ductility was estimated by Welch and Sullivan (2017) for each record in each building. Structural ductility values for the steel MRF buildings were estimated based upon the elastic strain energy, or "work-done", developed in the plastic hinge zones of the steel members. Structural ductility values were estimated for the RC wall buildings using the ratio of the maximum recorded displacement to the corresponding yield displacement, at the effective building height. Further details on the structural models are given by Welch (2016).

3 THE CURRENT NEW ZEALAND DESIGN STANDARD APPROACH

The design of parts or components to resist seismic demands is currently prescribed in *Section Eight Requirements for Parts and Components* of the New Zealand Standard NZS 1170.5:2004 with 2016 amendments (Standards New Zealand, 2016a) using a floor response spectrum approach, that appears to have been developed from Shelton (2004). This approach separates the ground motion intensity, amplification of demands with building height, part or component period, and the effects of nonlinear response of the part or component into individually approximated parameters, as shown in Figure 3.1. The various coefficients in this approach are described in the subsections that follow.

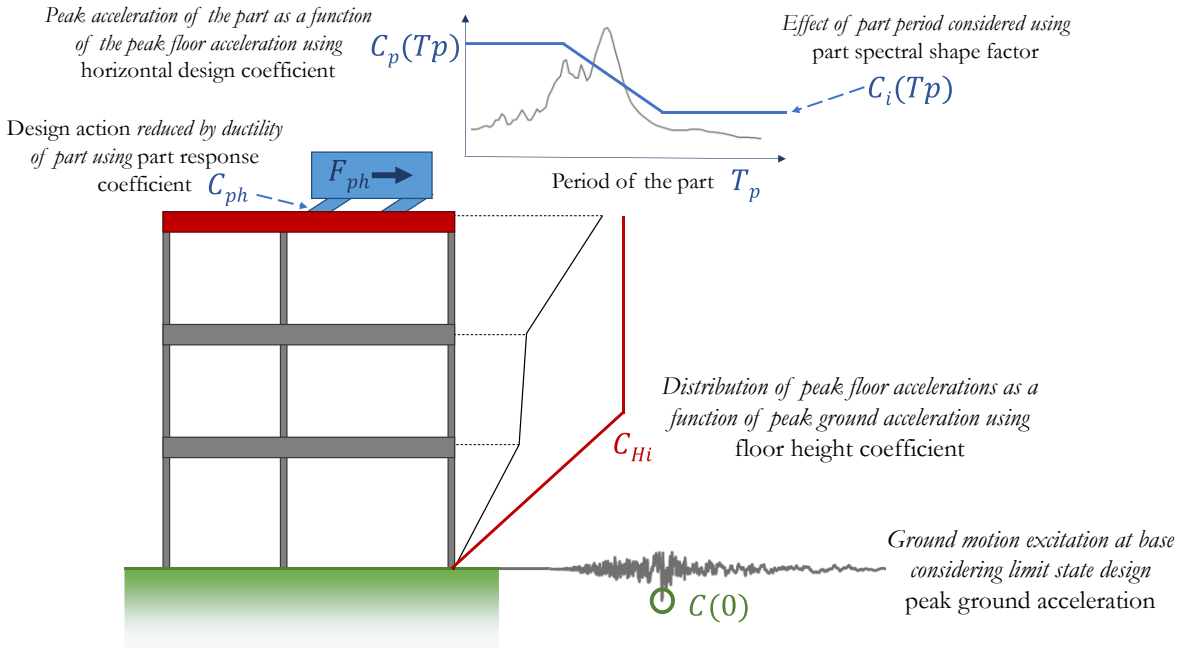

Figure 3.1: Summary of the NZS 1170.5 approach for estimating seismic demands on parts and components.

3.1 General Equation for the Horizontal Design Actions on Parts and Components

The horizontal design earthquake action on the part or component, F_{ph}, is determined using Equation 3.1:

$$F_{ph} = C_p(T_p)C_{ph}R_pW_p \leq 3.6W_p \tag{3.1}$$

Where $C_p(T_p)$ is the horizontal design coefficient of the part, which varies as a function of the period of the part, T_p; C_{ph} is the part horizontal response coefficient; R_p is the part risk factor, given as 1.0 for all cases except for where the consequential damage caused by its failure is disproportionately great; and W_p is the weight of the part. $C_p(T_p)$ is calculated using Equation 3.2:

$$C_p(T_p) = C(0)C_{Hi}C_i(T_p) \tag{3.2}$$

Where $C(0)$ is the peak ground acceleration, C_{Hi} is the floor height coefficient for level i, and $C_i(T_p)$ is the part spectral shape factor.

3.2 Floor Height Coefficient

The floor height coefficient captures the variation of peak floor acceleration (PFA) with floor height. This appears to have been introduced from the enveloped peak floor acceleration responses computed from the analytical modelling and instrumented building data described by Shelton (2004), which appears to generally follow the floor height amplification shape developed for reinforced concrete wall buildings by Rodriguez *et al.* (2002). The factor is a function of the height of attachment of the part, h_i, and the height from the base of the structure to the uppermost seismic weight or mass, h_n. For elevations that satisfy the height limitations of multiple lines, the lesser value of C_{Hi} is taken. This approach appears highly conservative (Uma *et al.*, 2010). This coefficient is shown in Figure 3.2, and computed using Equation 3.3.

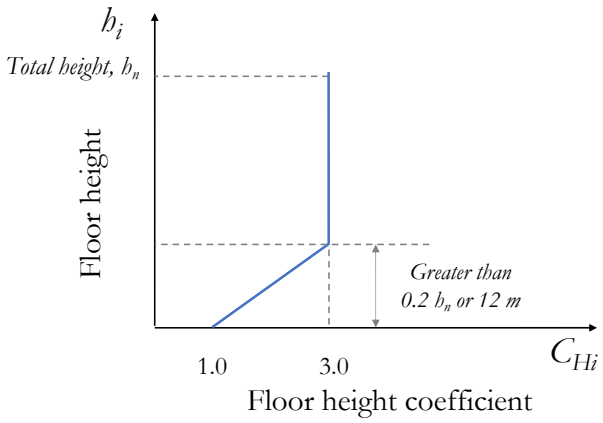

Figure 3.2: The floor height coefficient, C_{Hi}, in NZS 1170.5.

$$C_{Hi} = \begin{cases} 1 + \dfrac{h_i}{6} & \text{for all } h_i < 12 \text{ m} \\ 1 + 10\dfrac{h_i}{h_n} & h_i < 0.2h_n \\ 3 & h_i \geq 0.2h_n \end{cases} \tag{3.3}$$

The performance of the floor height coefficient is examined against the observed distributions of peak floor accelerations, normalised by the corresponding peak ground accelerations, of the case study instrumented buildings in Figure 3.3. The low-rise GNS Avalon Unit 2, possessing a relatively short fundamental structural modal period, is well approximated with the linearly-increasing floor height coefficient. With increasing building heights, and subsequently lengthening fundamental structural modal periods, the floor height coefficient appears to become more conservative, particularly at lower levels.

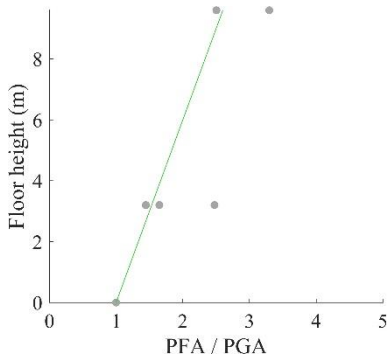

(a) GNS Avalon Unit 2 | Longitudinal

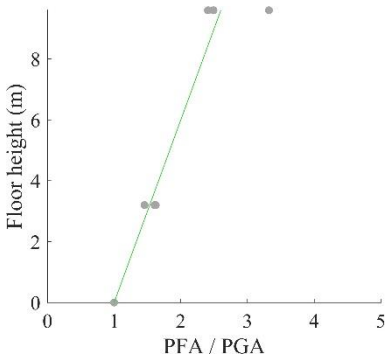

(b) GNS Avalon Unit 2 | Transverse

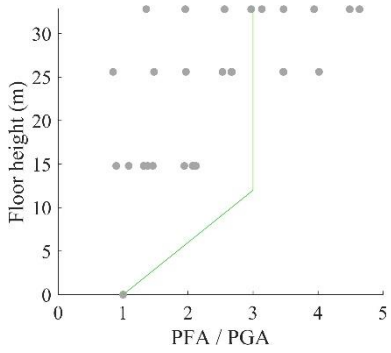

(c) UC Physics Building | Longitudinal

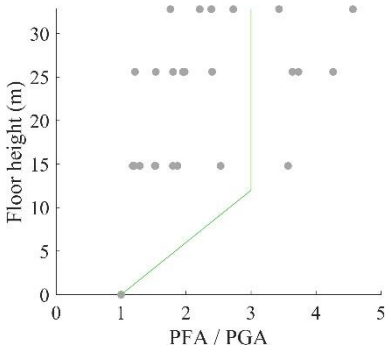

(d) UC Physics Building | Transverse

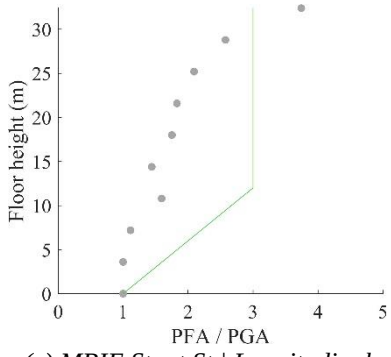

(e) MBIE Stout St | Longitudinal

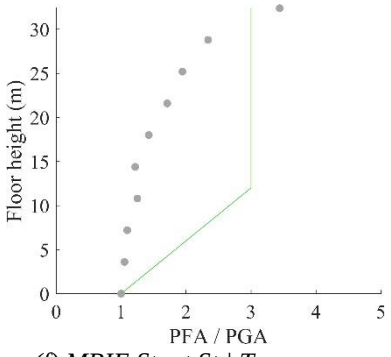

(f) MBIE Stout St | Transverse

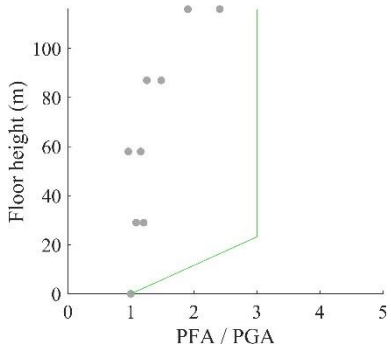

(g) Majestic Centre | Longitudinal

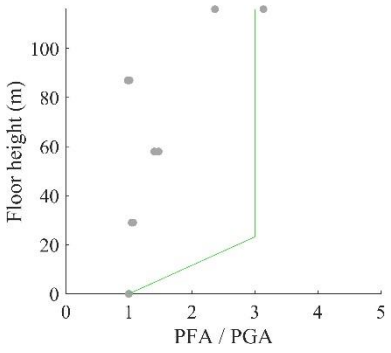

(h) Majestic Centre | Transverse

Figure 3.3: Distribution of peak floor accelerations, normalised by corresponding peak ground accelerations, in instrumented case study buildings. The current floor height coefficient, C_{Hi}, is shown.

Structural nonlinearity, developed through material inelasticity or geometric nonlinearity, has been widely observed to reduce peak floor accelerations (Aragaw, 2017; Buccella *et al.*, 2021; Haymes, 2022; Sullivan *et al.*, 2013; Vukobratović and Fajfar, 2017; Welch and Sullivan, 2017). Sullivan *et al.* (2013) explain that this is because once the resistance is reached, the force and acceleration that can be transferred by the fundamental structural modal response is limited. The current NZS 1170.5 approach does not explicitly consider this advantageous behaviour, and the floor height coefficient consequently over-estimates the distribution of peak floor accelerations induced during strong motions that result in nonlinear structural response.

The influence of structural nonlinearity on peak floor acceleration distribution, and the corresponding predictions from NZS 1170.5, is demonstrated in Figure 3.4. The median of the peak floor accelerations, normalised by the corresponding peak ground accelerations, is shown for the reinforced concrete wall and steel moment resisting frame buildings for motions that resulted in effective structural ductility values of 0.5, 1.0, 2.0, and 4.0, (the determination of which is described in Section 2) considering the results within 15% of the effective structural ductility estimations. The floor height coefficient is significantly conservative, particularly for the tallest buildings. The peak floor accelerations can be observed to generally decrease, relative to the corresponding peak ground accelerations, as structural inelasticity increases, which NZS1170.5 does not explicitly account for using the floor height coefficient.

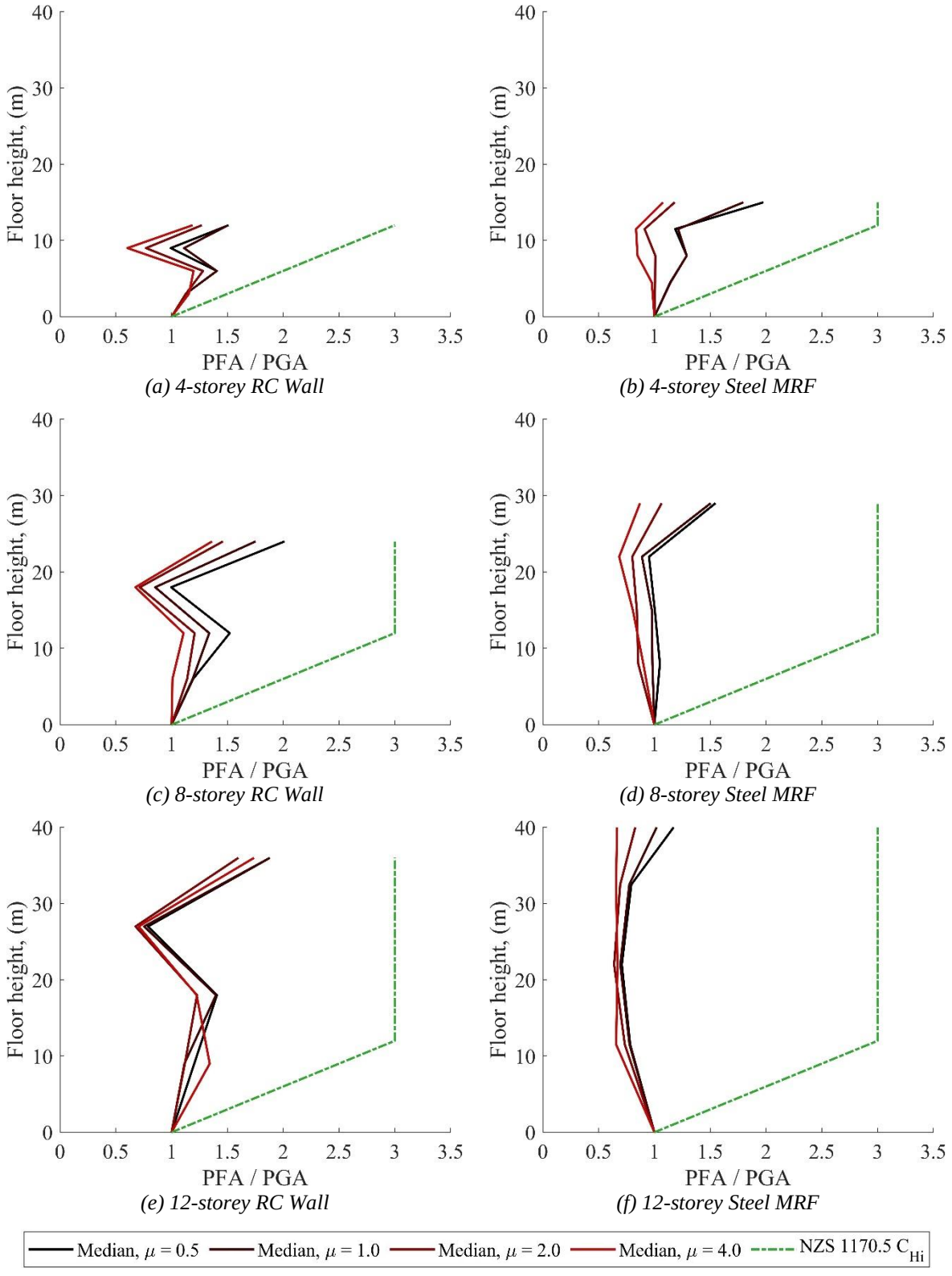

Figure 3.4: Distribution of peak floor accelerations, normalised by corresponding peak ground accelerations, for the six numerical case study buildings, at four effective structural ductility values. The current floor height coefficient, C_{Hi}, is shown.

3.3 Part Spectral Shape Factor

The part spectral shape factor, $C_i(T_p)$ has a trilinear shape which varies as a function of the period of the part. This factor envelopes the floor response spectrum shape that was considered typical at the time (Shelton, 2004). The factor is independent of the modal periods of the structure and has been observed to consequentially underestimate demands on flexible components with periods near long fundamental structural periods (Uma *et al.*, 2010). This factor amplifies the peak floor acceleration by two, although no amplification develops in rigid components, and thus appears over-conservative (Filiatrault and Sullivan, 2014; Sullivan *et al.*, 2013; Uma *et al.*, 2010). This possibly reflects code-writers' perceptions that very few components will be truly rigid, and, to avoid negative impacts associated with a designer underestimating the real period of a component, the demands at zero period are set to reflect those more likely at short periods. This approach is also over-conservative at very long part or component periods, and results in unrealistic corresponding relative displacement demands (Uma *et al.*, 2010). The part spectral shape factor is shown in Figure 3.5, and described in Equation 3.4:

$$C_i(T_p) = \begin{cases} 2 & T_p \leq 0.75\ s \\ 2(1.75 - T_p) & 0.75\ s < T_p < 1.25\ s \\ 0.5 & 1.25\ s \leq T_p \end{cases} \quad (3.4)$$

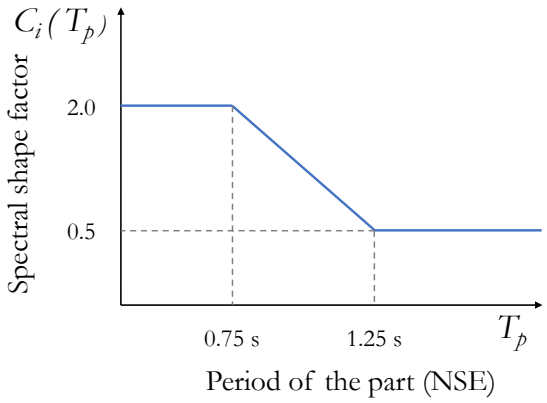

Figure 3.5: The part spectral shape factor, $C_i(T_p)$, in NZS 1170.5.

Figure 3.6 shows roof acceleration response spectra normalised by the corresponding peak floor accelerations, PFA, computed from motions recorded in the case study New Zealand instrumented buildings. These spectra were computed for damping ratios of the part or component of 1%, 2%, 5%, and 10%. The part spectral shape factor can be observed to under-estimate the peak spectral accelerations, which occur near resonance with the range of modes exhibited by these buildings, and significantly increase with decreasing damping values. Although it can be observed that parts with very short periods (i.e.: rigid parts) do not experience demands significantly greater than the peak floor acceleration, the part spectral shape factor doubles this value. The demands for parts and components with long periods can also be observed to be significantly over-predicted.

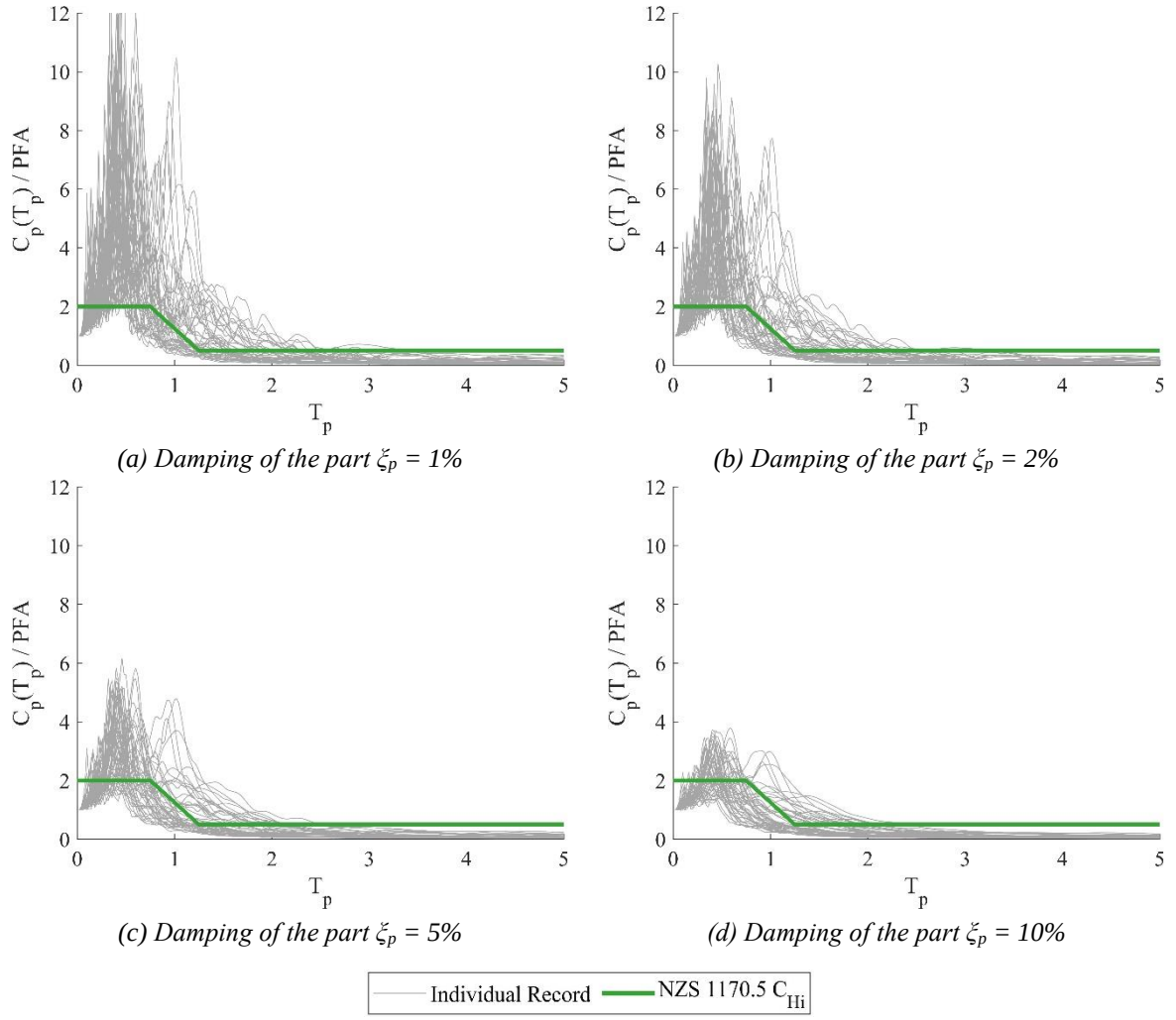

Figure 3.6: The roof spectral accelerations, $C_p(T_p)$, normalised by the corresponding peak floor accelerations, *PFA*, computed at four values of damping of the part or component, from motions recorded in seven instrumented buildings in New Zealand (GeoNet, 2022). The current part spectral shape factor, $C_i(T_p)$, is shown.

The floor acceleration response spectra shown in Figure 3.6 were computed from buildings that exhibited elastic response during the recorded motions. The formulation of the spectral shape factor by Shelton (2004), however, was based upon observations from numerical and instrumented buildings that experienced ductility. Structural nonlinearity may reduce the demands associated with structural modes, with the effective reduction often reducing with the order of modes (Aragaw, 2017; Haymes, 2022; Maniatakis *et al.*, 2013; Vukobratović & Fajfar, 2017; Welch & Sullivan, 2017). Consequently, the spectral shape factor better describes the expected higher mode amplification with the value of 2.0 and that expected for the fundamental period with the value of 0.5. Significant structural nonlinearity is not expected at the serviceability limit state (SLS) intensity, however, at which the NZS 1170.5 approach for estimating the demands on parts and components is often applied.

3.4 Part Response Factor

The part response factor, C_{ph} reduces the demands at all part periods with increasing part ductility. The part response factor does not have a clear rational basis for rigid components, for which no amplification is observed, and therefore, dynamic amplification effects are not reduced. This somewhat counteracts the conservative dynamic amplification prescribed at short periods of the part spectral shape factor if the ductility of the part is sufficient. The values for this factor are given in Table 3.1.

Table 3.1. Part response factor, C_{ph}, used in NZS 1170.5 (Standards New Zealand, 2016b).

Ductility of the part μ_p	Part response factor C_{ph}
1.0	1.0
1.25	0.85
2.0	0.55
3.0 or greater	0.45

The part response factor is used as a coefficient to reduce the demands computed using Equation 3.1. This may instead be considered as a reduction factor by computing the inverse of the part response factor. Figure 3.7 shows the Median reduction factors using the GNS Avalon, UC Physics, and the MBIE Stout St instrumented building records. Inelastic spectra were computed using INSPECT (Carr, 2016) for part damping values of 2%, 5%, and 10% at part ductility values of 1.2, 1.5, 2.0 and 3.0, applying a constant damping ratio coefficient retaining the initial elastic value and using an elastic-perfectly plastic hysteresis. An integration time step of 0.001 seconds was adopted.

The reduction corresponding to the NZS 1170.5 part response factor shown in Figure 3.7 can be observed to over-estimate the reductions over short periods, particularly for rigid parts. However, the reductions associated with flexible parts are significantly under-predicted. The greatest reduction occurs near resonance between the part and the fundamental modal period of the structure, with greater reductions occurring with lower values of part damping. These reductions are proportional to the dynamic amplification occurring near the structural modes, which is shown in Figure 3.6 to also increase with decreasing part damping values. Reductions are approximately equal to the ductility of the part where the period of the part is sufficiently longer than the fundamental structural modal period, at approximately 1.75 T_p / T_1, independent of the damping of the part.

The product of the part response factor and the part spectral shape factor characterises the influence of the dynamic response of the part or component on the demands on the part or component. The underlying simplifications from which these provisions were developed may result in reasonably well estimated floor response spectra if the structure and the part or component develop significant nonlinear response, as often anticipated at the ultimate limit state, but does not appear to adequately describe behaviours observed at lower intensities, as may be expected at the serviceability limit state. There appears to be an opportunity to update the provisions in NZS 1170.5 to better reflect the behaviours demonstrated in this section and to permit more explicit consideration of factors that influence demands on parts and components by engineering practitioners.

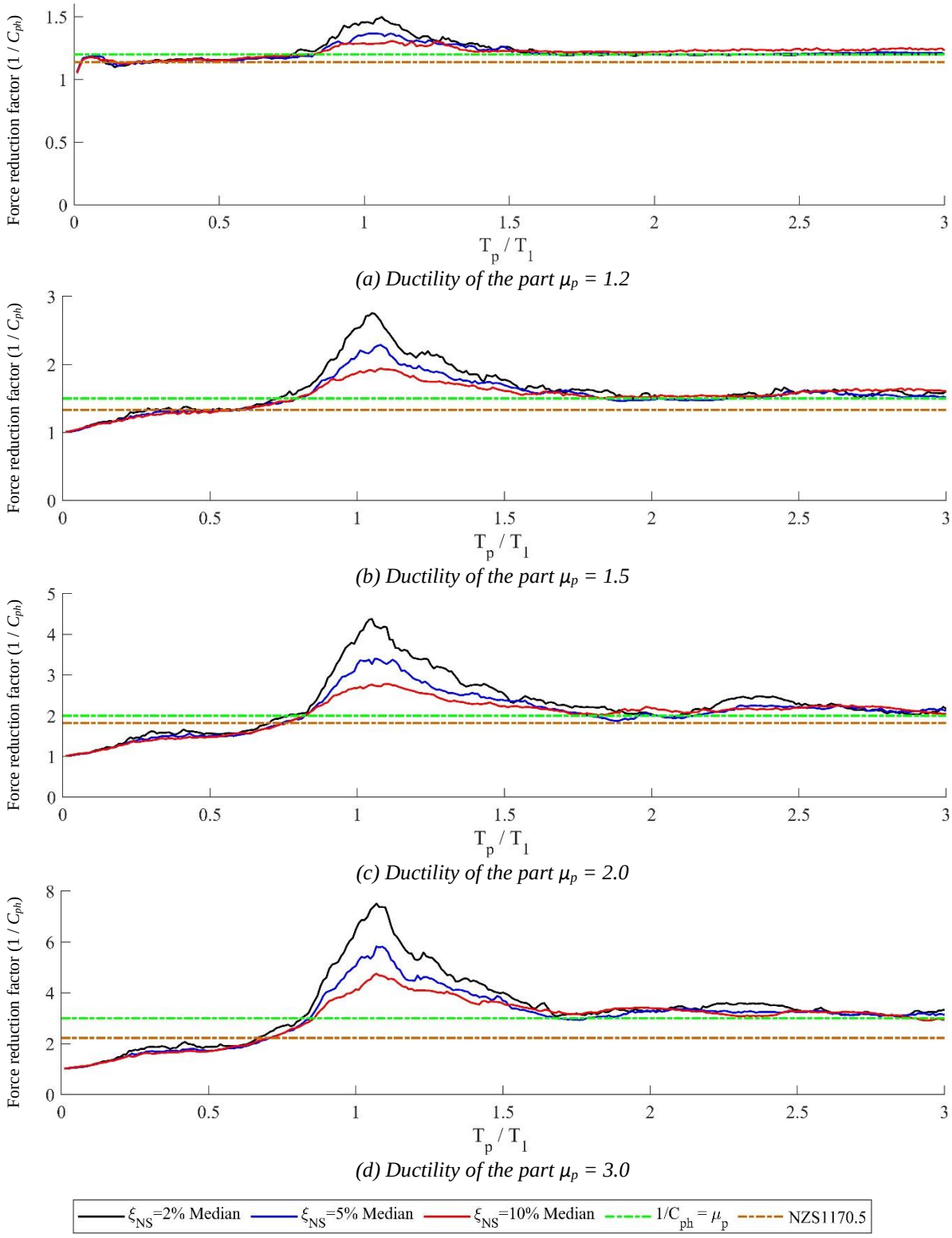

Figure 3.7: Median force reduction factors using instrumented building records. Inelastic spectra were computed at part damping values of 2%, 5%, 10% for allowable part ductility values of 1.2, 1.5, 2.0 and 3.0 using an elastic-perfectly plastic hysteresis. The inverse of NZS 1170.5 part response factor is shown.

4 THE ASCE/SEI 7-22 APPROACH

In the United States of America, the design of non-structural components to resist seismic demands is prescribed by ASCE/SEI 7-22 Minimum Design Loads and Associated Criteria for Buildings and Other Structures (American Society of Civil Engineers, 2021) and is based upon proposals by the Applied Technology Council (ATC, 2018). This approach approximates the ground motion intensity, the amplification of demands associated with structural and non-structural responses. Structural and non-structural responses are separated into simple amplification terms which rely on tables and basic equations. A summary of this approach is shown in Figure 4.1. The various parameters in this approach are described in the subsections that follow.

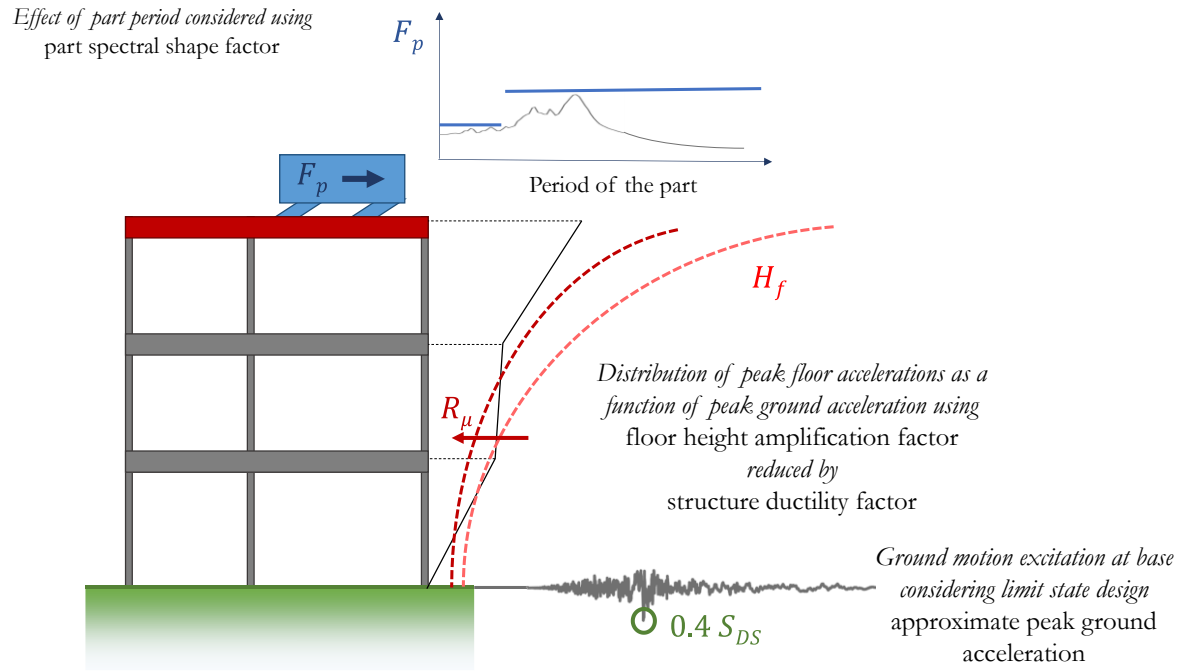

Figure 4.1: Summary of the ASCE 7-22 approach for estimating seismic demands on parts and components.

4.1 General Equation for the Horizontal Design Actions on Parts and Components

The force on the component, F_p, is determined using Equation 4.1:

$$F_p = 0.4\,S_{DS} I_p W_p \left[\frac{H_f}{R_\mu}\right]\left[\frac{C_{AR}}{R_{po}}\right] \tag{4.1}$$

Where the product of 0.4 and S_{DS}, the short-period design ground spectral acceleration, provides an approximation of the peak ground acceleration as a measure of ground motion intensity; I_p is the component importance level; W_p is the component weight; H_f is the factor for floor height amplification; R_μ is the structure ductility factor; C_{AR} is the component resonance ductility factor, which converts the

peak motion at the location of mounting to a peak component response; and R_{po} is the component strength factor.

4.2 Floor Height Amplification Factor

The factor for floor height amplification, H_f, defines how the peak ground acceleration is amplified to the floor levels of the structure based upon both the recorded variation in the peak floor acceleration, normalised by peak ground acceleration, in instrumented buildings in California and the mean (average) variation computed in simplified continuous models of a flexural beam laterally coupled with a shear beam (ATC, 2018). This is estimated as a function of the ratio of the height of the floor of interest, z, and the total building height, h, using Equation 4.2:

$$H_f = 1 + a_1\left(\frac{z}{h}\right) + a_2\left(\frac{z}{h}\right)^{10} \tag{4.2}$$

The variables a_1 and a_2 are functions of the shortest fundamental period of the building of any orthogonal direction, T_a, as given in Equations 4.3 and 4.4.

$$a_1 = \frac{1}{T_a} \leq 2.5 \tag{4.3}$$

$$a_2 = \left[1 - \left(\frac{0.4}{T_a}\right)^2\right] \geq 0 \tag{4.4}$$

The peak floor acceleration is assumed to increase linearly from 1 to 3.5 for structures with fundamental structural modal periods below 0.4 s, where the limits of Equations 4.3 and 4.4 are reached. There are reductions for buildings with greater periods. This is the most conservative distribution of demands, and is permitted to be used if the fundamental period of the building is unknown. The vertical distribution of demands reduces with longer fundamental structural modal periods. The distributions of demands with floor height prescribed by the ASCE 7-22 and NZS 1170.5 are compared in Figure 4.2.

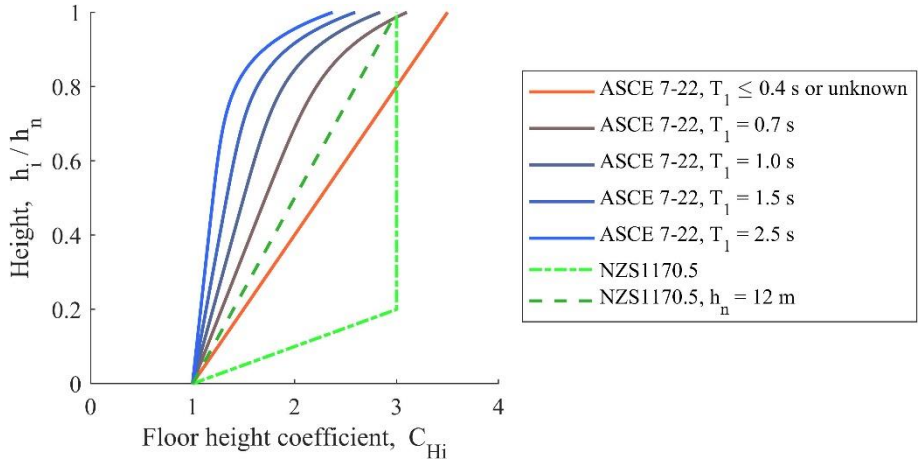

Figure 4.2. ASCE 7-22 and NZS 1170.5 provisions for the distribution of demands with floor height for different first modal periods, T_1.

The ASCE 7-22 factor for floor height amplification is applied for the four case study instrumented buildings in Figure 4.3. The factor appears to accurately describe the peak floor acceleration distributions, which are normalised in this figure by the corresponding peak ground acceleration. The demands at the roof of the GNS Avalon Unit Two building appear to be more conservatively predicted than the approach in NZS 1170.5. This does not appear to be a significant change, however, as the distribution of demands with floor height for short buildings varies from 1 to 3, if the maximum building height is 12 m (though less if the building height is shorter), using the NZS 1170.5 approach, and from 1 to 3.5 using the ASCE 7-22 approach. For taller buildings, with correspondingly longer fundamental periods, the distribution of demands with floor height appears to be far more closely predicted using the provisions in ASCE 7-22 than those in NZS 1170.5, particularly over lower levels. The wide dispersion of demands in the UC Physics Building data, in Figures 4.3c and 4.3d, indicate the large level of uncertainty in the estimation of demands with height that has been observed elsewhere (ATC, 2018; Miranda and Taghavi, 2009; Shelton, 2004). Although it is acknowledged that this is a limited data set, the instrumented building data presented here supports the observations made by ATC (2018) and Miranda and Taghavi (2009).

The peak floor acceleration distribution over the lower half of the structure adopted in ASCE 7-22 is significantly lower than the provisions in NZS1170.5 for buildings with a total height of greater than 12 metres. This seems to be due to the assumption by NZS1170.5 that higher structural modal response will result in very large amplifications over these lower levels. This assumption appears to be based upon the an envelope of peak floor acceleration distributions computed from the results of time history analysis of three reinforced concrete structures by Shelton (2004). There, peak floor accelerations are normalised by the elastic hazard, $C(0)$, instead of the peak ground acceleration of each record. Other studies considered herein (ATC, 2018; Drake & Bachman, 1995; Fathali & Lizundia, 2011; Miranda & Taghavi, 2009) which have examined results from numerical analysis and data from instrumented buildings have not observed the same significant amplifications over these lower levels.

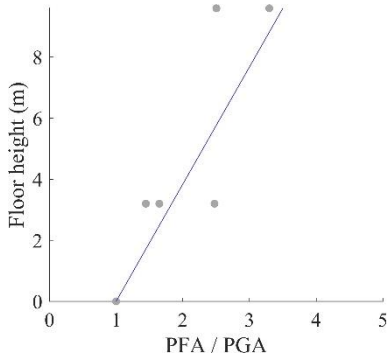

(a) GNS Avalon Unit 2 | Longitudinal

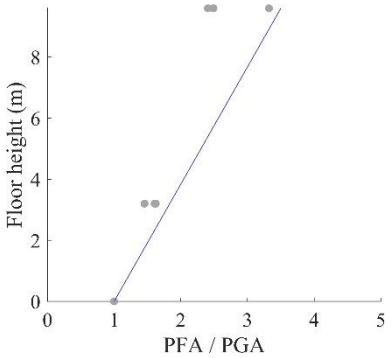

(b) GNS Avalon Unit 2 | Transverse

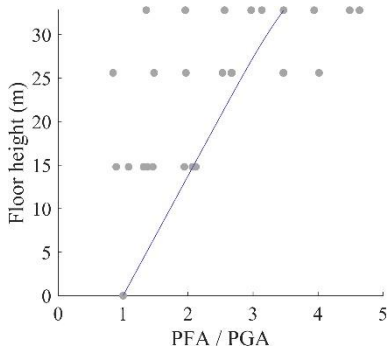

(c) UC Physics Building | Longitudinal

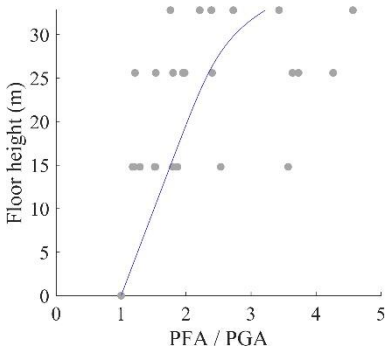

(d) UC Physics Building | Transverse

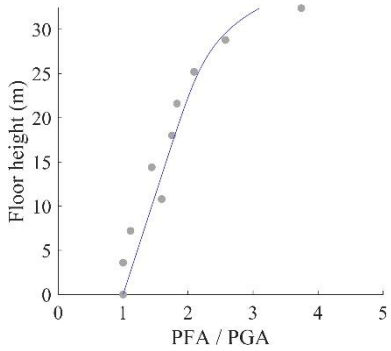

(e) MBIE Stout St | Longitudinal

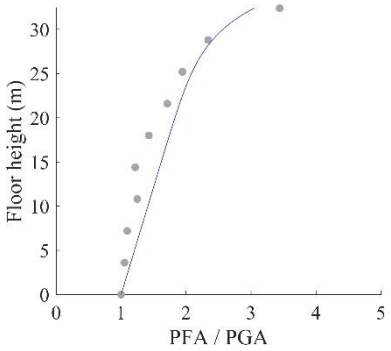

(f) MBIE Stout St | Transverse

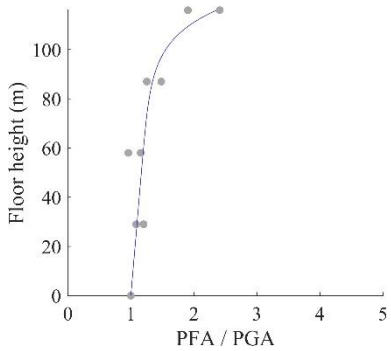

(g) Majestic Centre | Longitudinal

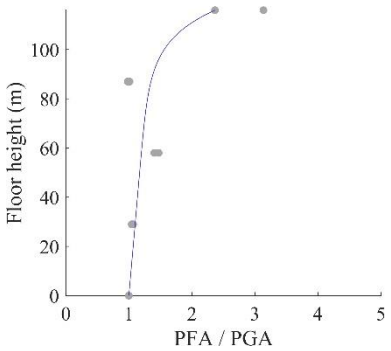

(h) Majestic Centre | Transverse

Figure 4.3: Distribution of peak floor accelerations, normalised by corresponding peak ground accelerations, in instrumented case study buildings. ASCE 7-22 factor for floor height amplification is shown.

4.3 Structure Ductility Factor

The floor height amplification, for components mounted above ground level, is reduced by the structure ductility factor, R_μ, as given in Equation 4.5.

$$R_\mu = \left[\frac{1.1\,R}{I_e \Omega_0}\right]^{0.5} \geq 1.3 \tag{4.5}$$

Where I_e is the importance factor of the building, specified in Section 11 of ASCE 7-22; R is the response modification factor for the building, and Ω_0 is the overstrength factor for the building, both specified for different lateral load resisting systems in a table in Section 12 of ASCE 7-22. This, therefore, implicitly considers the demands at high intensities that result in the given structural nonlinearity. The ATC-120 report, the origin of this factor, also permits the consideration of structure ductility factor as equal to the square root of the global ductility coefficient, R_D, (elsewhere referred to as μ) of the structure at the design earthquake level.

The structure ductility factor is applied at all levels of the building which results in non-conservative estimations of the forces over the lower half of the structure. This seemingly contradicts the assumed amplification of forces due to the response of the structure supporting the part that is described by the floor height amplification factor, which prescribes low amplifications of demands with height over the lower levels of the building, particularly for buildings with longer fundamental periods of vibration. This effect can be observed in Figure 4.4, which shows the influence of structural nonlinearity on peak floor acceleration distribution, and the corresponding predictions from ASCE 7-22, computed as the ratio of the floor height amplification factor and the structure ductility factor, [H_f / R_μ]. The median of the peak floor accelerations, normalised by the corresponding peak ground accelerations, is shown for the reinforced concrete wall and steel moment resisting frame buildings for motions that resulted in structural ductility values of 1.0, 2.0, and 4.0, considering 15% uncertainty in the estimation of the structural ductility estimations. The shape of the peak floor acceleration distribution appears poorly predicted over the lower half of the structures, with approximately linearly decreasing demands with lower floor levels, which can be observed to meet the lower bound limit of 0.75 PGA.

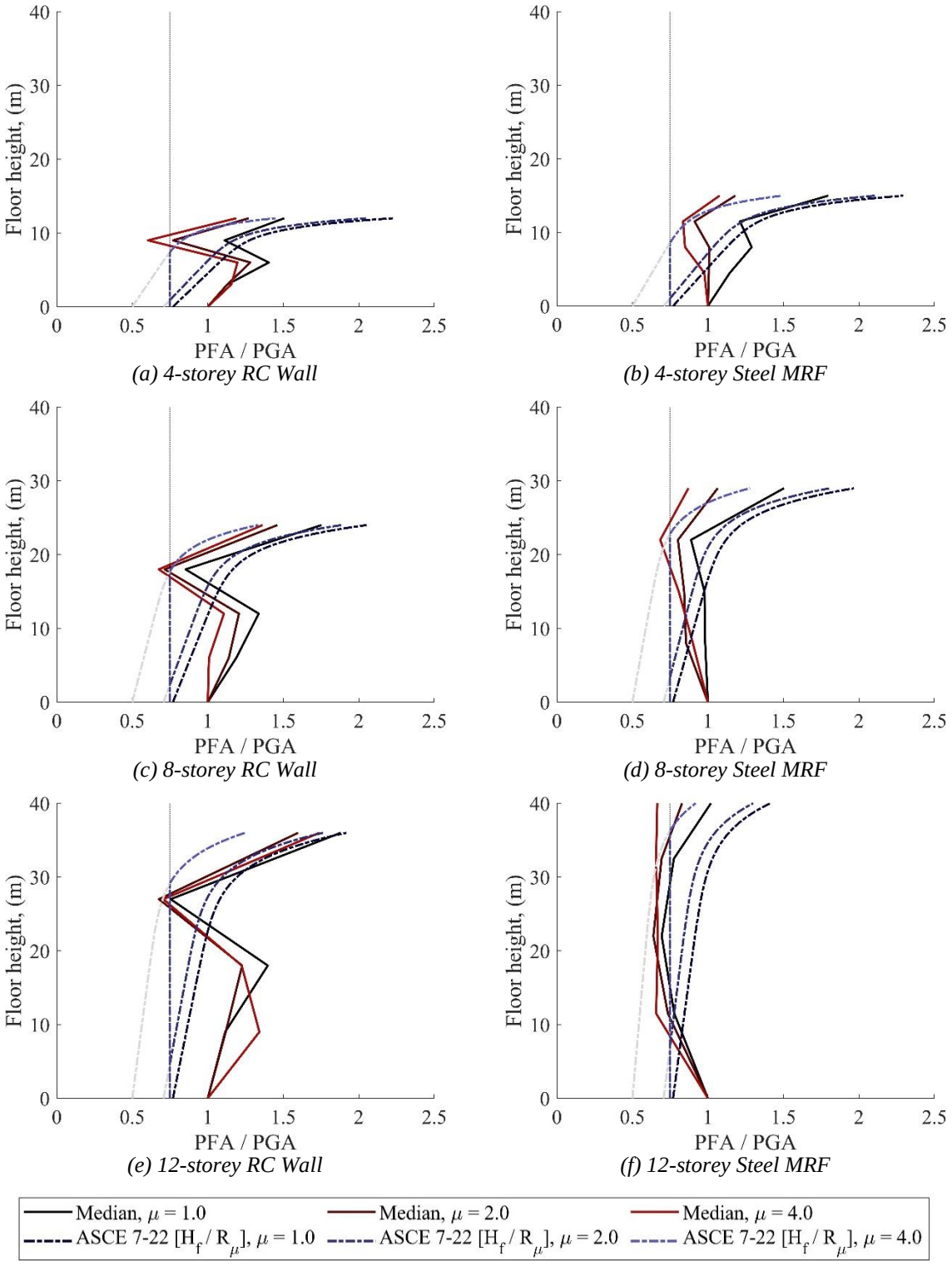

Figure 4.4: Distribution of peak floor accelerations, normalised by corresponding peak ground accelerations, for the six numerical case study buildings, at three structural ductility values. The floor height distributions predicted using ASCE 7-22, [H_f / R_μ], are shown.

The lateral load resisting system, reinforced concrete moment resisting frames, of the GeoNet-instrumented BNZ CentrePort building developed a significant inelastic response during the 2016 Kaikōura earthquake. Figure 4.5 shows the application of the elastic provisions from NZS1170.5 and ASCE 7-22. In the longitudinal direction, a reduction proportional with height can be observed. In the transverse direction, however, the recorded PFA/PGA amplification was greatest at roof level in the largest earthquake, but not over the lower levels. The results may be because greater nonlinear response developed in the longitudinal direction than the transverse. It would be beneficial to examine trends in the PFA/PGA relationships for a greater number of buildings responding inelastically, as part of future research.

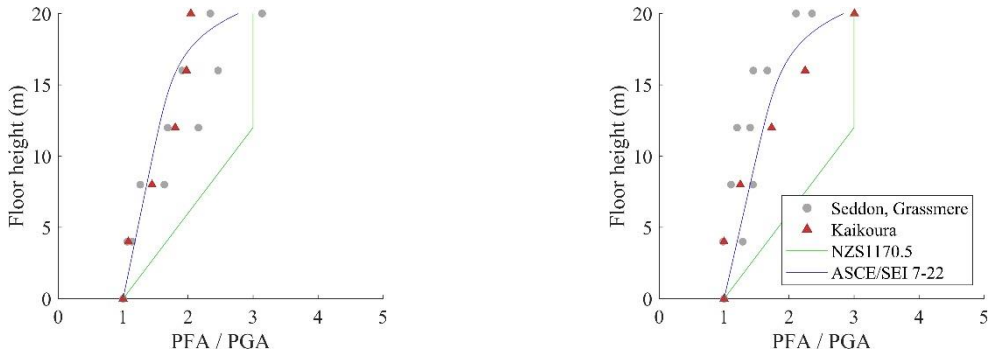

(a) Longitudinal *(b) Transverse*

Figure 4.5: Distribution of peak floor accelerations, normalised by corresponding peak ground accelerations, in the BNZ CentrePort building. The NZS1170.5 and ASCE 7-22 factors for floor height amplification are shown.

4.4 Component Resonance Ductility Factor

The amplification due to the response of the non-structural component, and subsequent apparent reduction from component nonlinearity, is given with the component resonance ductility factor, C_{AR}. This considers whether the component is likely to resonate with a structural mode, the degree of nonlinearity it can develop, and whether it is mounted on the ground or an elevated floor or roof. This removes the need for accurate estimation of non-structural and structural periods to assign dynamic amplification that is required by modal prediction methods. Values for the component resonance ductility factor and the component strength factor, R_{po}, are given in tables within the standard which were estimated using 5% non-structural damping. This was recommended by the ATC (2018) for consistency with the existing ASCE 7-16 methods (American Society of Civil Engineers, 2017), and it is noted therein that further research on non-structural damping is required, particularly at higher intensities (ATC, 2018).

4.5 Component Strength Factor

Values for the component resonance ductility factor and the component strength factor, R_{po}, are given in tables within the standard which were estimated using 5% non-structural damping.

4.6 Upper and Lower Bounds

ASCE 7-22 specifies upper and lower bounds for the seismic design force applied to parts and components. The demonstration of the application of these bounds is demonstrated in Figure 4.5.

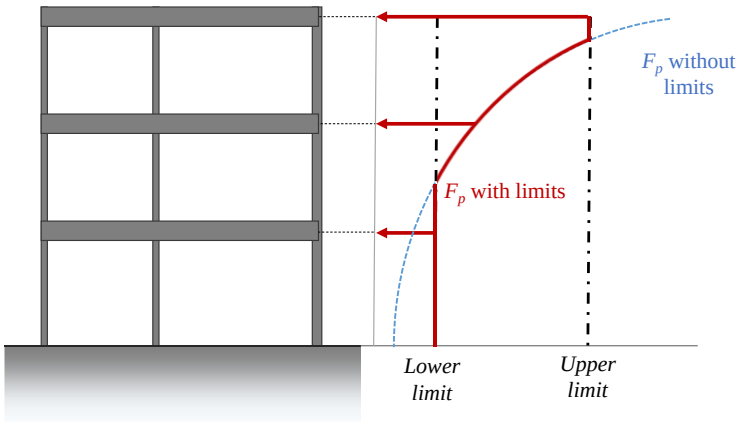

Figure 4.5: ASCE 7-22 lateral seismic design force on parts and components over building height.

4.6.1 Upper Bound

The upper bound for the seismic design force is given in Equation 4.6. The objective of this bound is to prevent the multiplication of individual factors to produce a design force that is thought to be unreasonably high. The application of this bound is based upon an expectation that the nonlinear response of the part or component and the supporting structure will significantly reduce demands on the part or component. As forty percent of the short period spectral acceleration, $0.4S_{DS}$, is assumed by the ASCE 7-22 approach to be approximately equal to the peak ground acceleration, the upper bound is approximately four times greater than the peak ground acceleration.

The ATC-120 report proposed to increase the maximum to $2.0S_{DS}$. This assumes the maximum demand occurs at the roof level ($z/H = 1$), all components exhibit some nonlinear capacity ($\mu_{comp} = 1.25$), and some structural nonlinearity. This was found to better approximate the values obtained from the primary design equation for some case study buildings with low structural ductility. The demands on components experiencing resonant behaviour with the structure in short rigid buildings were not enveloped, though this occurred for only a narrow band of component periods. The ATC-120 report recommends the use of greater component nonlinearity for this case.

$$F_p = 1.6\, S_{DS} I_p W_p \tag{4.6}$$

4.6.2 Lower Bound

The lower bound for the seismic design force is given in Equation 4.7. The lower bound in ASCE 7-22 is approximately equal to seventy-five percent of the peak ground acceleration. This minimum design

force was established in the 1991 Uniform Building Code [cite], and was subsequently adopted into ASCE/SEI 7. This bound considered the part or component mounted within the structure to experience 75% of the demands imposed at the ground level, and permitted a further reduction of two-thirds if mounted at the ground level, which was increased by a factor of 1.5 to convert from allowable stress design to strength design.

$$F_p = 0.3\, S_{DS} I_p W_p \tag{4.7}$$

The ATC-120 report (ATC, 2018) provided additional justifications for this lower bound. Rigid components mounted at the ground level experience the peak ground acceleration, and experience an actual strength approximated to be a factor of 1.3 lower than the design strength, providing the value for the force, normalised by the component weight and importance factor, of $0.31S_{DS}$. The lower bound for non-rigid components in the ATC-120 report uses the ASCE 7-16 provisions, and estimates an amplification of 2.5, and a component reduction of 3.0, resulting in a bound of $0.33S_{DS}$. The approach developed in ATC-120, however, considers a component amplification of 1.4 for flexible ductile components mounted at the ground level, and a component overstrength of 1.3, resulting in a lower bound of $0.43S_{DS}$

5 JUNE 2022 WORKSHOP WITH ENGINEERING PRACTITIONERS AND ACADEMICS TO REVIEW PARTS AND COMPONENTS PROVISIONS IN NEW ZEALAND

5.1 Overview of the Workshop

An all-day workshop to discuss the seismic demands on building parts and components was conducted on the 2nd day of June, 2022. The workshop was well attended by five academics and nine engineering practitioners, including three members of the NZ Seismic Risk Working Group. The workshop was successful in highlighting options for revision to the Parts & Components approach. However, agreement on what revisions should be made was not reached. The work presented in the current report comprises some of the additional work deemed necessary to facilitate definition of new design provisions in the future.

The week before the workshop all participants were provided (via email) the ATC-120 report (ATC, 2018) that formed the background to the revision of the seismic design requirements for nonstructural components in Chapter 13 of ASCE 7-22 . Participants were asked to review Sections 4.2 of the report, which evaluated the influence and importance of parameters that impact the seismic demands on parts and components, and Section 4.3, which proposed the approach later adopted in ASCE 7-22.

The workshop was structured to introduce key findings from research through a series of presentations. Participants were encouraged to contribute during discussion sessions throughout the workshop. The six presentations were conducted using a combination of existing literature and novel research conducted at the University of Canterbury.

Current code approaches and general issues were first presented. This was followed by a general discussion of potential benefits/drawbacks of any revisions to the parts and components approach. The data that was used to undertake much of the research presented during the workshop was outlined. Seismic demands on rigid parts and components were considered by a presentation on options for estimating peak floor accelerations. This topic was then opened for discussion. A presentation was delivered on insights into dynamic amplification from sprinkler testing from recent research conducted at the University of Canterbury. This provided an empirical basis for a presentation on acceleration amplification for non-rigid parts and components. This topic was then opened for discussion. A final presentation was given on other possible areas for revision to the parts and components approach. The workshop closed with a discussion session on all options for revision and future research needs.

High level discussions were held that included examining the need to improve seismic performance of parts of components; the balance of compromises between simplicity, specificity, and accuracy; cohesion between design standards; and previous considerations when prediction provisions have been developed.

Detail-oriented research questions were also raised. These included requests to obtain experimental evidence of behaviours, consideration of load paths, and the influence of hysteretic behaviour. These questions identify opportunities for further research to be conducted.

5.2 Outcomes from the Workshop

It appears that engineering practitioners consider the current NZS approach to be conservative. However, research has shown that the NZS approach can produce both conservative and non-conservative estimates, with non-conservative estimates being particularly likely in buildings with long fundamental periods, and for parts and components with low damping (Haymes et al., 2020; Uma et al., 2010; Welch & Sullivan, 2017). There is limited evidence that components experience the demands associated with low damping values, however. The proposal in the ATC-120 report limits the damping ratio value of parts and components to five percent, based upon the limited characterisation of parts and components that is currently available, particularly at high intensities.

Prediction methods have been developed considering the superposition of the effects of the modal response of the structure, which have been observed to significantly alter floor response spectra, determining the amplitude of amplified demands, and the periods of the parts at which this occurs (Aragaw, 2017; Haymes et al., 2020; Merino et al., 2020; Vukobratović & Fajfar, 2017; Welch & Sullivan, 2017). However, practitioners attending the workshop were hesitant for the design standards to require modal analysis. The current NZS1170.5 standard is independent of the fundamental structural modal period, which practitioners expressed a desire to maintain. This was based on their notion that the fundamental structural modal period cannot be estimated easily and reliably by users of the standard. This opinion was held despite the explicit use of this parameter in the design procedures for parts and components in Eurocode 8 (European Committee for Standardization, 2004) and ASCE/SEI 7-22 (American Society of Civil Engineers, 2021). To this extent, any practice-oriented method should make allowance for uncertainty in the estimation of structural modal periods, as considered by Haymes et al. (2020).

Some workshop attendees expressed scepticism about the large demands associated with the amplification of the dynamic response of parts and components with periods near structural modal periods in elastic floor acceleration response spectra. This was based in a belief that most parts and components have an inherent ability to develop nonlinearity to reduce these demands. This is perhaps reflective of the commentary to NZS1170.5, where all parts and components, except for glazing, are estimated to develop nonlinear responses at the design ultimate limit state. By permitting even small part ductility values, large reductions for components with periods near resonance of the supporting

structure have been demonstrated (Applied Technology Council, 2018; Haymes, 2022; A. K. Kazantzi et al., 2020; Vukobratović & Fajfar, 2017). Greater guidance could be developed on how part ductility can be achieved, either through bolt slip, material inelasticity, rocking, or other means, and the degree of nonlinearity that is required to be developed to acquire the desired response.

The current NZS1170.5 approach for estimating parts & components acceleration demands can be applied with greater ease and speed than modal superposition approaches. The provision of multiple means for compliance, permitting practitioners to determine demands using methods of varying complexity, was discussed in the workshop, where it was noted that multiple approaches are permitted for the determination of seismic loads on structural elements by NZS1170.5. The evolving computational ability of technology was suggested to reduce the significance of computational expenditure, particularly for methods that require relatively few parameters. The adoption of a modal superposition floor response spectrum approach in practice may, therefore, be facilitated by software, an application, or an online tool.

The prediction provisions developed in the ATC-120 project and subsequently adopted in ASCE 7-22, outlined in the previous section, were discussed during the workshop. Attendees acknowledged what appears to be a robust basis for the ASCE7-22 provisions. Consistent with the existing framework of NZS1170.5, practitioners favour the ability to explicitly consider the influence of first-principle parameters for design, such as the non-structural ductility, to enable more diverse design options. The attendees were reluctant to adopt prescribed values for specific components from tables.

The current code approach does not explicitly consider floor displacement response spectra. The spectral shape factor provides a constant value of 0.5 for non-structural periods greater than 1.25s, resulting in unrealistically large spectral displacement demands at long periods. This limits the ability for practitioners to estimate the relative displacement demand on non-structural elements. This may be important for checking clearance requirements, which is common for designing suspended services like distributed sprinkler systems.

Perhaps most importantly, New Zealand engineering practitioners expressed a strong desire for a strong rational basis to be provided to the design approach for non-structural elements that is adopted in future standards. This desire may be interpreted as a mandate for future research into the seismic performance of parts and components, but it is also clear that current knowledge should be used to update existing provisions.

6 RECOMMENDED REVISIONS TO THE NEW ZEALAND DESIGN STANDARD

In light of the discrepancies highlighted in Section 3, the recent developments made in the United States in ASCE 7-22 discussed in Section 4, and the workshop findings outlined in Section 5, revisions for estimating the seismic demands on parts and components are recommended. However, revisions should seek to maintain the existing NZS 1170.5 framework and minimise alterations where possible to facilitate its adoption by practicing New Zealand engineers. The objective of this section is to identify how the current parts and components procedure can best be updated so that it is reliable and simple to use, founded with a robust scientific basis. The recommended approach is shown in Figure 6.1. The various parameters in this approach are described in the subsections that follow.

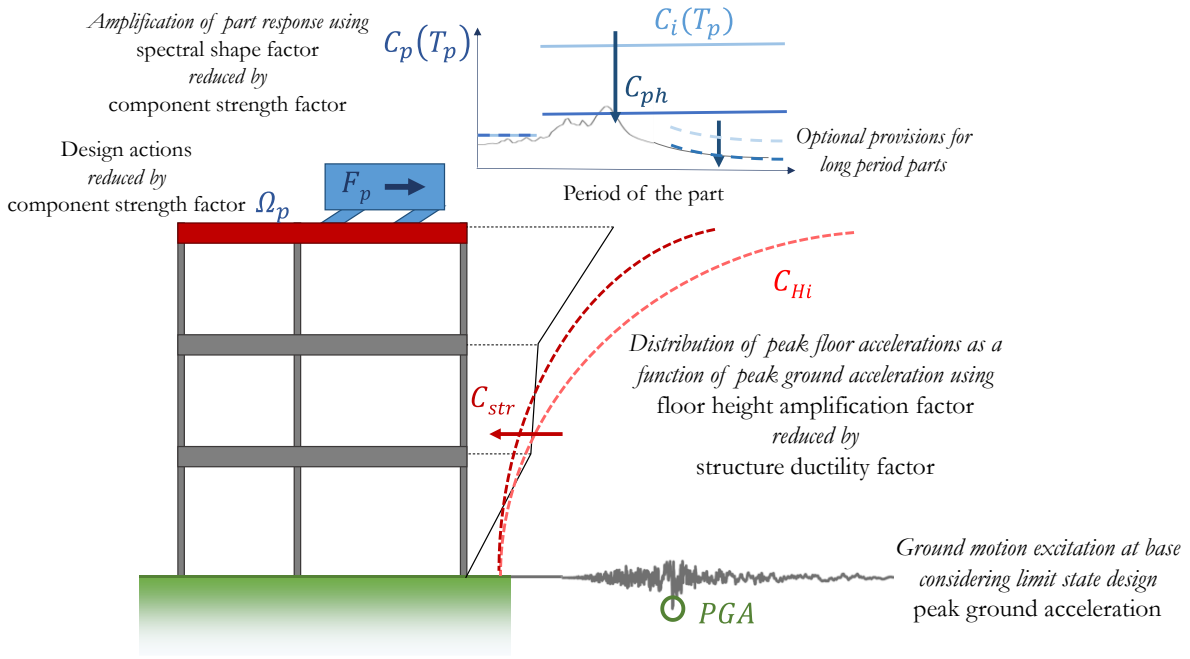

Figure 6.1: Summary of the recommended approach for estimating seismic demands on parts and components.

6.1 General Equation for the Horizontal Design Actions on Parts and Components

It is recommended that the general equation from NZS1170.5 for the horizontal design earthquake actions on a part, F_{ph}, be determined from Equation 6.1:

$$F_{ph} = \frac{C_p(T_p)}{\Omega_p} R_p W_p \leq 5.0\, PGA\, W_p \tag{6.1}$$

Where $C_p(T_p)$ is the horizontal design coefficient of the part; Ω_p is the component overstrength factor, which is recommended as 1.5 unless demonstrated to be greater; R_p is the part risk factor, given as 1.0

for all cases except for where the consequential damage caused by its failure is disproportionately great; W_p is the weight of the part; and *PGA* is the peak ground acceleration, using the variable name that is consistent with new provisions in Section 3 of NZS 1170.5. The recommended design force expression in Equation 6.1 differs from the existing expression in Equation 3.1 by removing the part response factor coefficient. This instead is suggested to appear earlier in the design process with the recommended design response coefficient for parts, $C_p(T_p)$, in Equation 6.2, in a similar form as in ASCE 7-22 (Equation 4.2).

$$C_p(T_p) = PGA\left[\frac{C_{Hi}}{C_{str}}\right]\left[\frac{C_i(T_p)}{C_{ph}}\right] \tag{6.2}$$

Where C_{Hi} is the floor height coefficient for level i, C_{str} is the structural nonlinearity reduction factor, $C_i(T_p)$ is the part or component spectral shape coefficient, and C_{ph} is the part or component horizontal response factor. The form of this equation may be considered as describing the effect of the ground motion intensity with *PGA*, the modification of *PGA* to a peak acceleration of the considered floor (*PFA*) by the building response, and the modification of *PFA* to a peak part or component acceleration by the response of the part or component. Recommendations for the quantification of these components are provided in the subsections that follow.

6.2 Ground Motion Intensity

The effects of ground motion intensity are quantified in Equation 6.2 using the peak ground acceleration at the considered design hazard. This is consistent with the existing NZS1170.5 approach, but differs from the approach adopted in ASCE 7-22. There, an effective peak ground acceleration is used approximated as the average spectral acceleration ordinates over the design short period range, the short period spectral acceleration, S_{DS}, factored by 0.4. This is thought to better describe the structural response and damage potential of an earthquake by eliminating the effects of high frequency ground responses (Feinstein & Moehle, 2022).

Modal superposition methods for the estimation of floor acceleration response spectra (Aragaw, 2017; Haymes, 2022; Merino et al., 2020; Vukobratović & Fajfar, 2017; Welch & Sullivan, 2017) approximate the demands associated with dynamic behaviour of parts and components due to structural modal responses using the ground spectral accelerations associated with each considered structural mode, in each considered orthogonal loading direction. These approaches consider the product of the ground spectral accelerations and factored mode shapes of each structural mode. The ground motion intensity is therefore approximated considering the ground spectral accelerations of each mode, and may be best described by the often-dominant first structural modal response. This may not be well represented by short period spectral accelerations for tall and/or flexible buildings.

The use of peak ground acceleration to describe ground motion intensity is recommended because the recommended revisions for the floor height coefficient, discussed next, relies on the expressions calibrated by the Applied Technology Council (2018) using peak floor accelerations normalised by the

corresponding peak ground accelerations that were recorded in instrumented buildings in the United States. Indeed, the ATC-120 2018 report proposed using $0.4S_{DS}$ as an approximation of the peak ground acceleration until it is explicitly used in future editions of ASCE 7. Further, maintaining consistency with the existing NZS1170.5 provisions is thought to facilitate adoption of the recommended revisions.

6.3 Floor Height Coefficient

The recommended floor height coefficient at level i, C_{Hi}, should be determined from Equation 6.3. This is adopted directly from ASCE 7-22, where Equations 4.3 and 4.4 have been substituted into Equation 4.2:

$$C_{Hi} = 1 + \frac{1}{T_1}\left(\frac{h_i}{h_n}\right) + \left[1 - \left(\frac{0.4}{T_1}\right)^2\right]\left(\frac{h_i}{h_n}\right)^{10} \tag{6.3}$$

Where h_i is the height of attachment of the part from the base of the structure, and h_n is the height from the base of the structure to the uppermost seismic weight or mass in the structure. T_1 is the largest translational period of vibration of the primary structure in the direction being considered, and not to be taken to be less than 0.4 s. If T_1 is equal to or less than 0.4 s, or unknown, the floor height coefficient can be calculated using the simple form in Equation 6.4. This, therefore, accounts for the limits specified in ASCE 7-22 (Equations 4.3 and 4.4).

$$C_{Hi} = 1 + 2.5\left(\frac{h_i}{h_n}\right) \tag{6.4}$$

The application of Equation 6.4 for single-storey structures results in a floor height coefficient at the roof of 3.5. This is significantly greater than the current NZS1170.5 approach, which gives a floor height coefficient of 1.6 for a building height of 3.6 m. A structure that may reasonably be modelled as a single-degree-of-freedom system with a short period, as expected for single-storey building, may be expected to experience the constant acceleration region of the design ground response acceleration spectrum, which will be referred to as the short period spectral acceleration, S_{AS}, in the upcoming revision of the New Zealand design standard. Consequently, the theoretical floor height coefficient may be described as the ratio of the short period spectral acceleration, S_{AS}, to the peak ground acceleration, PGA, determined considering the local seismic hazard. This approach will be conservative for single-storey buildings with periods greater than those associated with the short period spectral acceleration.

The estimation of the largest translational period of vibration of the primary structure in the direction being considered, referred to as the fundamental period for brevity, permits the use of lower floor height coefficient values using Equation 6.3 over the more conservative Equation 6.4, provided the estimated period is greater than 0.4 s. Equation 6.4 acts as an upper bound, therefore permitting the use of the recommended provisions without requiring any knowledge of the modal characteristics of the structure. Many simplified empirical expressions for approximating the fundamental period of structures have been developed, including the approach adopted in Section C4.1 of the commentary to NZS1170.5 (Standards New Zealand, 2016b). There, the fundamental period is approximated using the total height

the building and a coefficient configured for different lateral load resisting systems. This approach could be used in lieu of more robust estimates. The fundamental period of the structure may also be influenced by foundation and soil flexibility and by non-structural components, which are rarely modelled explicitly when estimating structural modal properties.

6.4 Structural Nonlinearity Reduction Factor

Several studies have demonstrated different amplitudes of the reduction of the peak floor acceleration distribution with height due to structural nonlinearity correspond to different structural vibrational modes, where the reduction is greatest in the fundamental structural mode and decreasing with the increasing order of modes, depending on the lateral force resisting system (Aragaw, 2017; Buccella, 2019; Haymes, 2022; Maniatakis et al., 2013; Vukobratović & Fajfar, 2017; Welch & Sullivan, 2017). Reductions are often approximated to be equivalent to the structural displacement ductility developed, with higher mode reductions neglected for simplicity.

The method recommended herein considers the effects of the structural response on the distribution of the peak floor accelerations, thereby approximating the combination of the structural modes using direct simplified expressions. The structure ductility factor from ASCE 7-22 is adopted here as the maximum structural nonlinearity reduction factor, as given in Equation 6.5:

$$C_{str,max} = \sqrt{\mu} \leq 1.3 \tag{6.5}$$

Where μ is the structural ductility factor. The lower bound value in Equation 6.5 of 1.3 assumes that all structures will develop the effects of nonlinearity at all considered design intensities, including sources of flexibility and nonlinearity within the structural joints, foundation and soil which may not often be explicitly modelled.

Figure 6.2 shows the reduction factors computed from the peak floor accelerations of all six case study numerical models of the reinforced wall and steel moment resisting frame buildings. The reductions were calculated by first computing the ratio of the peak floor accelerations (PFA) and corresponding peak ground accelerations (PGA) for all analysed motions, and comparing the PFA/PGA ratio computed at the lowest scaled peak ground acceleration for each of the forty-four ground motion records used, to the ratio computed at by scaling the corresponding motion to the six (RC) or seven (steel) considered peak ground acceleration intensities. Figure 6.2 shows the application of Equation 6.5. The reductions for low structural ductility values are over-estimated, but the numerical model does not consider the additional sources of nonlinearity discussed above. Reductions for greater ductility values appear to be reasonably approximated by Equation 6.5, although there appears to be significant variation in the computed reductions. Significant variation has also been observed in the elastic peak floor acceleration distributions (ATC, 2018; Drake & Bachman, 1995; Fathali & Lizundia, 2011; Miranda & Taghavi, 2009).

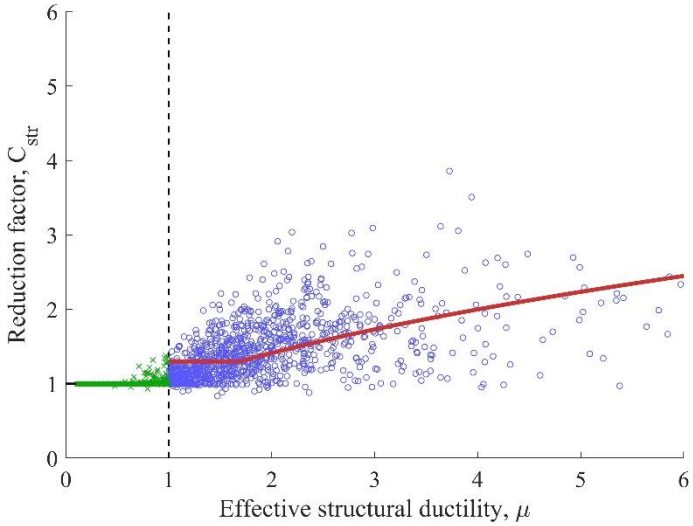

Figure 6.2: Structural nonlinearity reduction factors computed from the peak roof accelerations from the six case study numerical buildings. The recommended reduction factor, computed using Equation 5.5, is shown.

Figure 4.4 provides evidence that the reduction of the peak floor accelerations due to structural nonlinear response is not distributed equally with floor height. This may be anticipated considering the empirical correlation of reductions with structural modal response. Consequently, the structural nonlinearity reduction factor, C_{str} recommended here is determined from Equation 6.6 using the relative floor height through the floor height distribution exponent for structural nonlinearity reduction, e_{str}, given in Equation 6.7:

$$C_{str} = C_{str.max}^{\,e_{str}} \tag{6.6}$$

$$e_{str} = \left({}^{h_i}/_{h_n}\right)^{1.5} \tag{6.7}$$

where h_i is the height of attachment of the part from the base of the structure, and h_n is the height from the base of the structure to the uppermost seismic weight or mass in the structure.

Equation 6.6 is applied for parts and components above ground level, as the effects of structural inelasticity do not influence parts or components at or below ground level, where structural nonlinearity reduction factor can be taken as equal to 1.0. Conversely, the maximum reduction is expected to occur at the roof level, as reductions in the peak floor acceleration distribution are often dominated by the response of the first mode, which is expected to increase with floor height. These bounding characteristics are considered through this mathematical form, as the exponent, as e_{str} will be zero at the base, and one at the roof. The exponent that raises the relative floor height in Equation 6.7 defines the shape of the distribution of the reduction of peak floor accelerations.

Figure 6.3 shows the structural nonlinearity reduction factor distribution with height. The exponent that raises the normalised floor height in Equation 6.7, here shown as *x*, is varied and the adopted value of 1.5 is indicated. The lower levels of the building are not expected to experience significant reductions due to higher mode effects and the relatively low amplitude of the first structural mode. Using the value of 1.5 results in a reduction of approximately 30% of the maximum reduction at the mid-height. This appears to produce reductions similar to the peak floor acceleration distributions reported in many studies (Applied Technology Council, 2018; Kelly, 1978; Welch & Sullivan, 2017).

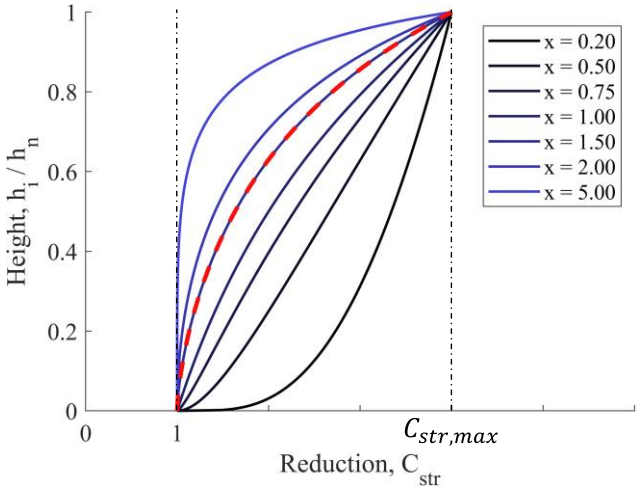

Figure 6.3: Structural nonlinearity reduction factor distribution with height. The exponent that raises the normalised floor height in Equation 6.7, here shown as *x*, is varied and the adopted value of 1.5 is indicated.

The application of this approach to the median peak floor accelerations of the case study numerical buildings, shown earlier in Figure 4.4, is presented here in Figure 6.4. The predicted peak floor accelerations exhibit "s" shaped distributions which appear to better approximate those observed from the results of numerical modelling than the approach in ASCE 7-22. This approach is significantly less conservative than the current NZS1170.5 approach for estimating the floor height distribution.

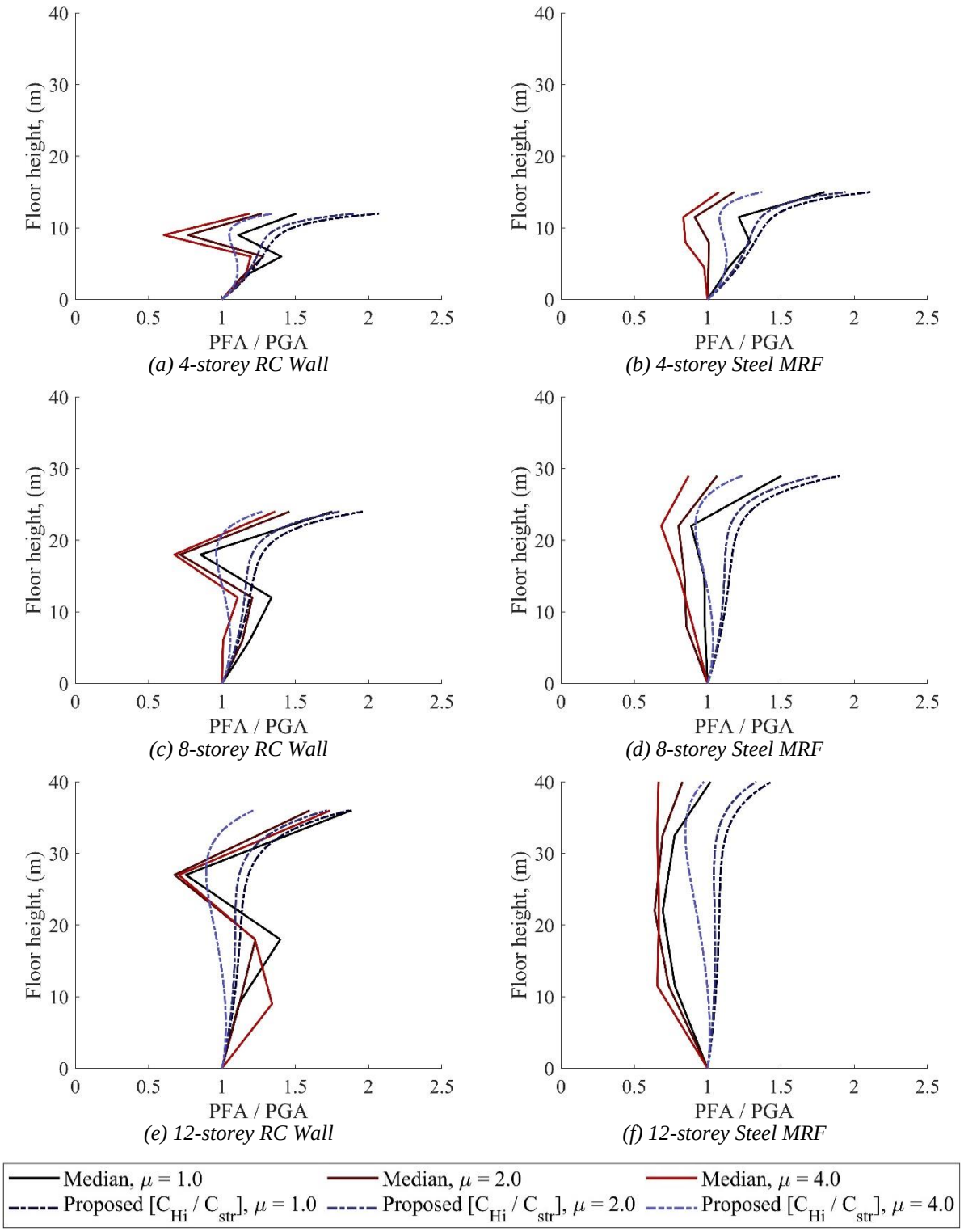

Figure 6.4: Distribution of peak floor accelerations, normalised by corresponding peak ground accelerations, for the six numerical case study buildings, at three structural ductility values. The floor height distributions predicted using the recommended provisions, [C_{Hi} / C_{str}], are shown.

6.5 Part or Component Spectral Shape Coefficient

The part or component spectral shape coefficient, $C_i(T_p)$, describes the maximum amplification anticipated for a part of component based upon its dynamic properties considering the elastic response of the part. The part or component spectral shape coefficient is given in Table 6.1.

Table 6.1: Part or component spectral shape coefficient, $C_i(T_p)$

Rigid parts or components	**Flexible parts or components**	
All levels	*At or below ground level*	*Above ground level*
1.0	$\frac{S_{AS}}{PGA}$	4.0

Where S_{AS} is the short period spectral acceleration, and *PGA* is the peak ground acceleration, as determined using the design ground motion hazard. This is used for parts mounted at or below ground level based on the assumption that the maximum elastic spectral acceleration that may be developed for parts mounted at or below ground level is equal to the constant short period spectral acceleration, S_{AS}. The design process for ground mounted parts considers the parameters that consider the effects of the structure, the floor height coefficient and the structural nonlinearity reduction factor, to be equal to one. Consequently, the maximum dynamic amplification that may be theoretically achieved using design ground acceleration response spectra, is equal to the ratio of the short period spectral acceleration and the peak ground acceleration. This approach will be conservative for parts with periods greater than those associated with the short period spectral acceleration.

6.5.1 Defining Rigid and Flexible Parts and Components

The definition of parts as rigid or flexible is a key challenge for the implementation of this approach. This approach was adopted in previous versions of ASCE 7, but was updated to match the ATC-120 classification based upon a likelihood of being in resonance with the fundamental mode of the building, defined using bounds of the ratio of the period of the part to the fundamental structural period of 0.5 to 1.5. The tabulated component resonance ductility factor, C_{AR}, appears to have to consider short and stiff buildings, with relatively short periods, resulting in the same rigid/flexible framework in previous versions. It is not clear how values in the tables that specify the component resonance ductility factors in ASCE 7-22 were formulated. The period ratio definition may also be unsatisfactory, as significant dynamic amplification associated with higher structural modes with periods shorter than half the fundamental period have been frequently observed (ATC, 2018; Aragaw, 2017; Buccella et al., 2021; Haymes et al., 2020; Kehoe & Hachem, 2003; Kelly, 1978; Vukobratović & Fajfar, 2017; Welch & Sullivan, 2017).

There are many complicating factors when approximating the period of the part. This includes sub-assemblies, nonlinearity resulting period elongation, connections, anchorage, and the presence of different vibrational properties in different loading directions (Feinstein & Moehle, 2022; Kehoe, 2014;

Watkins et al., 2010). It is also uncommon for practitioners to have reliable estimates of the period of parts. By classifying parts as rigid or flexible, the period of the part is not explicitly required.

Preliminary guidance on the classification of parts and components as likely rigid or flexible is provided in Appendix A, informed from the current commentary of NZS1170.5 and from ASCE 7-22. It is expected that future tables will undergo further review and revision in the future and are provided to show the intent of the recommended approach. The diversity of parts and components means a prescriptive approach to classification of parts as rigid or flexible with tables offers only limited insight into expected response. Classification of components using tables should be conducted with caution, as practitioners may inaccurately characterise components as rigid if they are unfamiliar with the relevant dynamics (Kehoe, 2014). Kehoe (2014) recommended providing some limitations to the parts that are assumed to be rigid, through the basis of dimensions or properties of the parts.

6.5.2 Maximum Dynamic Amplification

Characterisation of maximum dynamic amplification of a part or component has been investigated in several studies (eg: Biggs, 1971; Haymes, 2022; Sullivan *et al.*, 2013; Welch and Sullivan, 2017). Welch and Sullivan (2017) recommended a dynamic amplification factor considering the damping of the structural system, ξ_{str}, and of the part or component, ξ_p. By considering a range of SDOFs, an expression was derived using time-history analyses of single-degree-of-freedom representations of parts or components and their supporting structure at tuning (i.e. $T_p = T_1$). Using observations from instrumented building data, Haymes (2022) recommended lowering the maximum dynamic amplification factor from Welch and Sullivan (2017) using a coefficient of two-thirds, hypothesising that perfect tuning may not develop in real-world structures due to small variations in stiffnesses and material nonlinearity from cracking, joint flexibility, or other sources. The maximum part or component spectral shape coefficient for flexible parts and components mounted above ground level using the dynamic amplification factor from Haymes (2022) is given in Equation 6.8:

$$C_i(T_p) = \frac{2}{3}\left(0.5\xi_{str} + \xi_p\right)^{-\frac{2}{3}} \tag{6.8}$$

Experimental characterisation of mechanical parts and components by Watkins et al. (2010) observed damping values of between 0.5% and 5%, whereas other studies on contents and architectural parts and components observed damping values of between 9% and 30% (Marsantyo et al., 2000; Ryu et al., 2012; Tian et al., 2015). Despite these efforts, there remains limited characterisation of the damping of many parts and components, especially for the high ground motion intensities that are most relevant for design, where damping is expected to be greater. Consequently, this work follows the approach by ATC (2018) to consider a 5% damping value to derive amplification values. Equation 6.8 was applied using structural and part damping values of 5%, resulting in a part or component spectral shape coefficient of 3.75, supporting the use of the value of 4.0 in Table 6.1 for flexible components mounted above ground level.

Figure 6.5 shows the influence of part damping values on roof spectral accelerations, $C_p(T_p)$, normalised by the corresponding peak floor accelerations, PFA, computed at four values of damping of the part or component, from motions recorded in seven instrumented buildings in New Zealand (GeoNet, 2022).

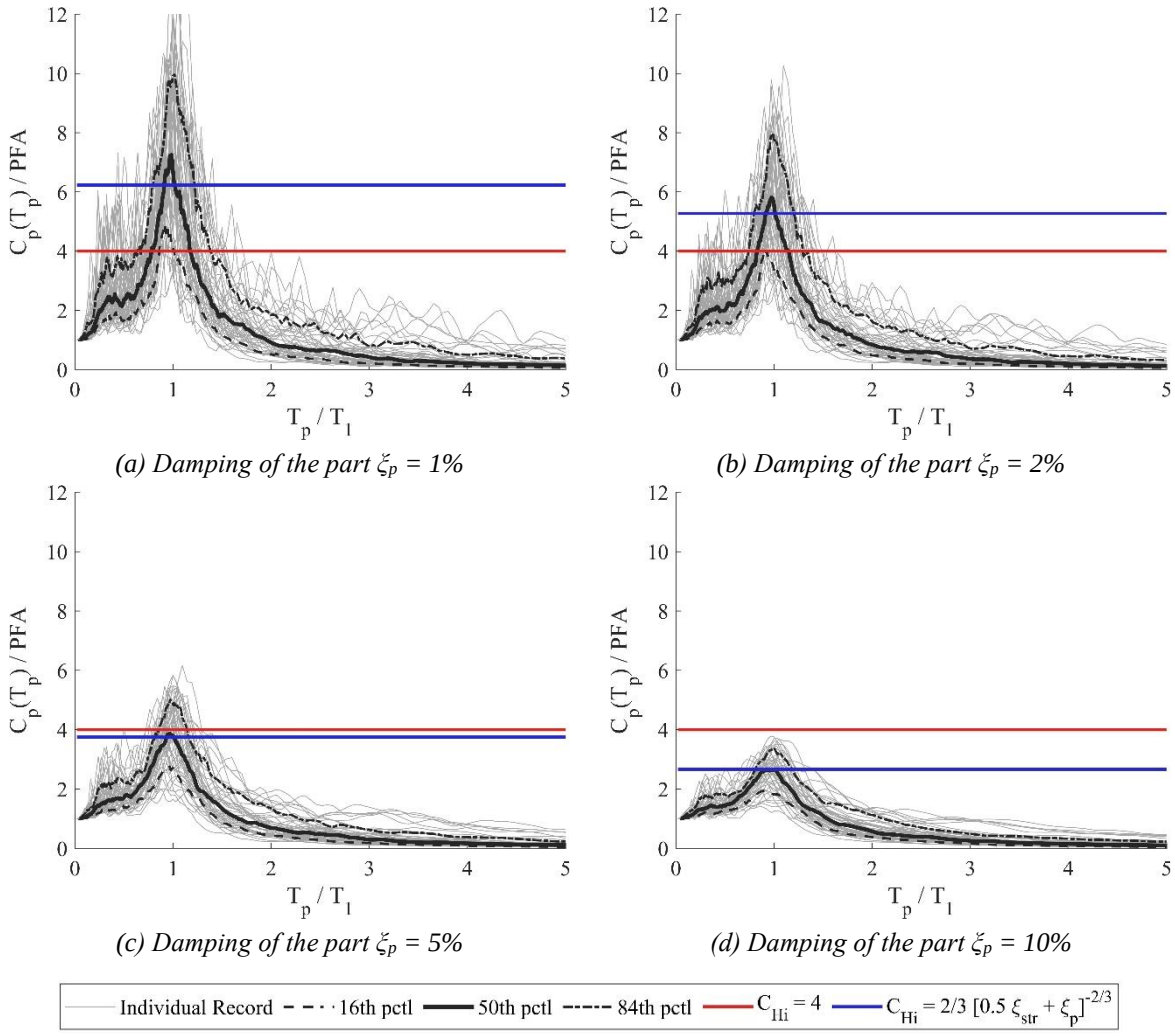

(a) Damping of the part ξ_p = 1%

(b) Damping of the part ξ_p = 2%

(c) Damping of the part ξ_p = 5%

(d) Damping of the part ξ_p = 10%

Figure 6.5: The roof spectral accelerations, $C_p(T_p)$, normalised by the corresponding peak floor accelerations, *PFA*, computed at four values of damping of the part or component, from motions recorded in seven instrumented buildings in New Zealand (GeoNet, 2022).

6.6 Part or Component Response Factor

The recommended part or component horizontal response factor, C_{ph}, should be determined using the values provided in Table 6.2. This follows the tabulated form of the part or component response factor in the current NZS1170.5 approach, but recommends some significant changes.

The current part or component response factor is used as a coefficient in the general design expression in Equation 3.1, and thus adopts values equal to or less than one, whereas the recommended approach suggests use of the part or component response factor as a reduction factor for the elastic amplification, described by the part or component spectral shape factor within the expression for design the response coefficient for parts, $C_p(T_p)$, in Equation 6.2, and thus has values equal to or greater than one.

The recommended part or component response factor distinguishes between rigid and flexible parts, whereas the current approach applies the coefficient for all parts, independent of the period of the part. Rigid parts are not expected to experience amplification nor reductions, and the term $[C_i(T_p)/C_{ph}]$ is equal to one in all cases. As shown and discussed in the previous subsection, elastic flexible parts and components may experience significant dynamic amplification, particularly if they have low damping. Using instrumented building data, including the results presented in Figure 3.7, Haymes (2022) proposed that the design yield force could be approximated to have a reduction equal to the permitted ductility of the part raised to the power of 1.5, $\mu_p^{1.5}$, for the dynamic amplification associated with the response of the part to the fundamental structural mode, and approximated it as equal to the permitted ductility of the part, μ_p, for dynamic amplification for higher structural modes, for parts with periods significantly greater than the fundamental structural mode, and for parts mounted at the ground level. The values computed using these expressions are rounded to the nearest 0.05 to provide the recommended part and component response factors in Table 6.2. These values are similar to those recommended in the ATC-120 report (2018).

Table 6.2: Recommended part or component response factor, C_{ph}.

Ductility of the part, μ_p	**Rigid parts** *All levels*	**Flexible parts**		**Long period parts**[1] *All levels*
		At or below ground level	*Above ground level*	
1.0	1.0	1.0	1.0	1.0
1.25	1.0	1.25	1.4	1.25
1.5	1.0	1.5	1.85	1.5
2.0	1.0	2.0	2.8	2.0
2.5 or greater	1.0	2.5	4.0	2.5

[1]A Long period part is taken as a part or component having a fundamental period, T_p, greater than $T_{p,long}$, where $T_{p,long}$ is defined in Section 6.8.

Part ductility may be developed through nonlinearity, either through material inelasticity or geometric nonlinearity like rocking, bolt slip, or sliding. The characterisation of part ductility values in the commentaries of NZS1170.5 and ASCE 7-22 are not explicitly supported with cited research and have instead relied upon judgement. These values are summarised in Appendix A. While both suggest shake table testing for verification, this may be of limited availability for the vast multiplicity of parts and

components. Table 6.3 provides generalised descriptions that may assist in the estimation of permissible ductility values. Characterisation of part ductility is an area of ongoing research.

Table 6.3: Generalised expected ductility values, μ_p.

Description	Part ductility, μ_p
All rigid parts or components	N/A
Flexible parts or components	
with good ductility capacity	2.5
with unknown but likely ductile behavior or slip capacity, or limited ductile capacity	1.5
with unknown and potentially brittle behaviour	1.25

6.7 Upper Bound of the Horizontal Design Force

The horizontal design earthquake actions on a part normalised by the weight of the part, F_{ph}/W_p, determined Equation 6.1, has a upper bound of 5.0 *PGA.* This is derived considering a flexible part with unknown and potentially brittle behaviour, corresponding to a part spectral shape factor of 4.0 and part response factor of 1.4, mounted at the roof of an elastic building with a short or unknown fundamental period, corresponding to a floor height coefficient, C_{Hi}, of 3.5 and structural nonlinearity reduction factor, C_{str}, of 1.3. These values correspond to a design response coefficient for parts, $C_p(T_p)$, of 7.69 *PGA*, which provides a F_{ph}/W_p, of 5.12 *PGA* if a component overstrength of 1.5 and a part risk factor of 1.0 is considered.

Figure 6.6 shows the ratio of the elastic 5%-damped roof level spectral accelerations of the considered New Zealand instrumented buildings to the corresponding peak floor acceleration, for part periods normalised by the buildings fundamental period. This figure is similar to Figure 4-38 in the ATC-120 report (2018) which was also developed using instrumented building data.

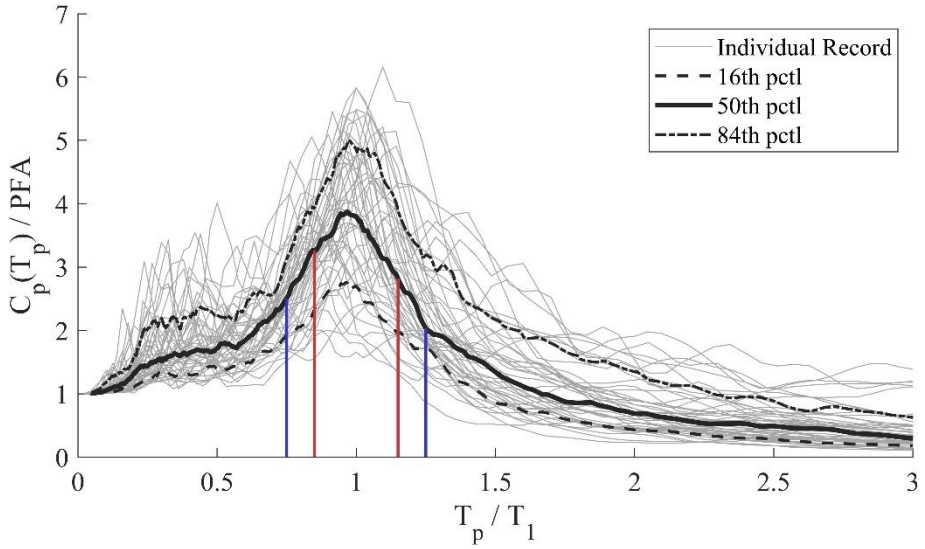

Figure 6.6: Ratio of the roof level spectral accelerations in New Zealand instrumented buildings to the corresponding peak floor acceleration, for part periods normalised by the buildings fundamental period.

Figure 6.6 shows that, if a part or component is near resonance with the fundamental structural modal period, significant dynamic amplification may occur. However, if the period of the part falls further from the fundamental period, here shown with bounds at 15% and 25%, the amplification significantly lessens. The balance of acceptable risk based upon the probability of resonant behaviour may justify the adoption of the limit of 5.0 PGA for all components, even for very brittle components or for low intensities where a part ductility of 1.25 is not permitted. Consider also that while NZS1170.5 currently limits the horizontal design force acting on parts and components to the weight of the part, W_p, factored by 3.6 in Equation 3.1, there does not appear to be a robust scientific basis for this limit.

Unlike ASCE 7-22, NZS1170.5 does not currently have a lower bound for the horizontal design force. The adoption of a lower bound within a revised New Zealand standard is not recommended, as no strong rationale for this was found within the present work.

6.8 Long Period Parts and Components

When the periods of the parts are much greater than those of the modes of building, the peak demands on the parts are correlated closely with those expected at the ground level, especially as the period of the part becomes greater. At these long periods, the relative motion from the modal response of the structure is not significantly influencing the response of the part. There is, however, a transition between parts with periods that are near the fundamental structural mode which exhibit responses that are primarily determined from the modal response of the structure, to parts that exhibit responses that are well approximated using the corresponding ground response spectrum.

It is recommended that long period parts and components should be defined as those possessing a period, T_p, that is greater than the threshold long period $T_{p,long}$, which may be determined as:

$$T_{p,long} = T_1\left(1 + \sqrt{\mu}\right) \tag{6.9}$$

Where T_1 is the largest translational period of vibration of the primary structure in the direction being considered, and μ is the structural ductility factor. Where the structure is expected to respond elastically, the threshold long period is equal to twice the fundamental structural period. Structural nonlinearity has been widely observed to result in the lengthening of the structural modal periods (ATC, 2018; Aragaw, 2017; Buccella et al., 2021; Calvi, 2014; Vukobratović & Fajfar, 2017) and was described by (Sullivan et al., 2013) and (Calvi & Ruggiero, 2017) to effectively produce a plateau of demands between the initial elastic and the elongated inelastic periods. Existing floor response spectrum prediction approaches often limit the influence of period elongation to the demands associated with the fundamental structural mode, approximating the elongation by a factor of the square-root of the structural ductility (Filiatrault & Sullivan, 2014; Sullivan et al., 2013; Welch & Sullivan, 2017), based on work by (Priestley et al., 2007). This has been observed to be conservative by other studies, which examined effective elongation fundamental periods (Calvi, 2014; Haymes, 2022) on spectral demands and hence the form adopted in Equation 6.9 is recommended.

If parts are found to have a period greater than the threshold long period using Equation 6.9, it is recommended that the design response coefficient, $C_p(T_p)$, be determined using Equation 6.10:

$$C_p(T_p) = \frac{S_a(T_p)}{C_{ph}}\left[1 + \frac{1}{\left(\frac{T_p}{T_1} - 1\right)^2}\right] \tag{6.10}$$

Where $S_a(T_p)$ is determined from the seismic hazard at the considered design level intensity in Section 3 of NZS1170.5, and C_{ph} is the part response factor. The expression within the square brackets accounts for the transition between parts with periods that are near the fundamental structural mode which exhibit responses that are primarily determined from the modal response of the structure, to parts that exhibit responses that are well approximated using the corresponding ground response spectrum, and follows the expression for the long period dynamic amplification factor proposed by Haymes et al., (2020), with similar expressions used in other modal superposition approaches (Vukobratović & Fajfar, 2017; Welch & Sullivan, 2017).

Figure 6.6 shows the ratio of the roof acceleration response spectra, computed at permitted part ductility values of 1.0, 1.5, and 3.0, to the corresponding elastic ground acceleration response spectra, for earthquake motions recorded in the instrumented GeoNet, MBIE, and UC Physics buildings. Recommended provisions for long period parts and components are indicated.

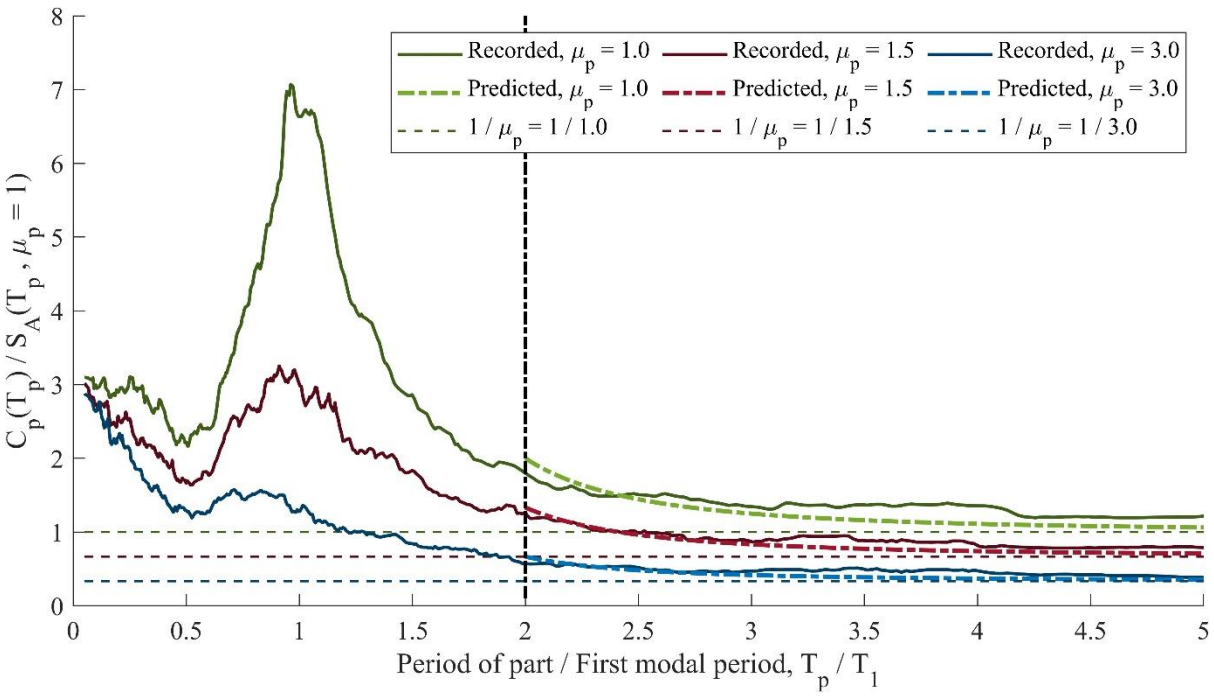

Figure 6.6: The ratio of the roof acceleration response spectra, computed at three part ductility values, to the corresponding elastic ground acceleration response spectra, for earthquake motions recorded in four New Zealand instrumented buildings. Recommended provisions for long period parts and components are indicated.

In Figure 6.6, the ordinates of 1.0 occur where the median inelastic floor spectral acceleration is equal to the elastic ground spectral acceleration. The dashed lines, indicating the inverse of the value of the permitted ductility of the part, corresponds to the application of the C_{ph} term in Equation 6.10, using the values specified in Table 6.2. It can be observed that the ratio of the inelastic floor to elastic ground spectral accelerations tends towards these values as the ratio of the period of the part to the period of the first structural mode for period ratios beyond 2.0, i.e.: the computed threshold long period for elastic building response. The transition between the spectral accelerations influenced by the first modal response of the structure, near a period ratio of 1.0, and those for very long period ratios, can be observed to be approximated using the expression in the square brackets of Equation 6.10.

Figure 6.7 shows the ratio of the roof to ground spectral accelerations computed using time history analysis of the 4-, 8-, and 12-storey reinforced concrete wall buildings by Welch and Sullivan (2017), corresponding to four effective structural ductilities. There, the recommended provisions for long period parts and components are indicated. The amplification associated with the response of the first structural mode, for period ratios near 1.0, can be observed to reduce with increasing structural inelasticity. The range of period ratios associated with the amplified response of the parts can be observed to occur over greater period ratios. The threshold long period is consequently lengthened, and the application of the provisions for long period parts appears to remain appropriate.

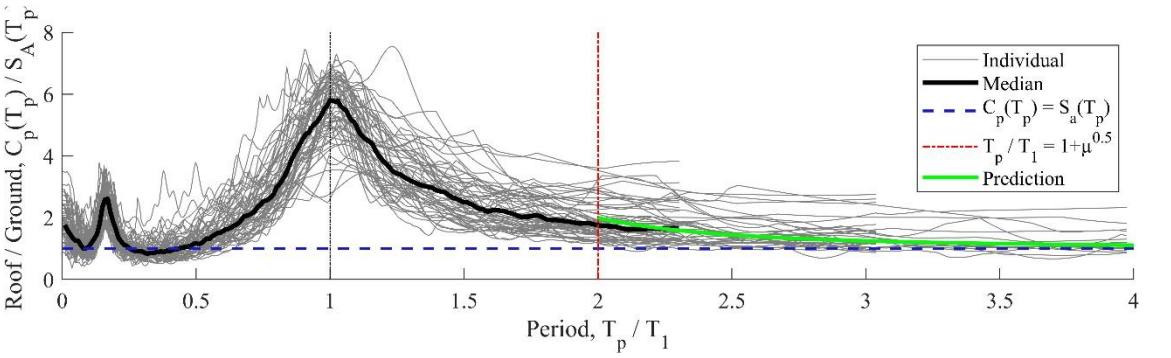

(a) Structural ductility μ = 0.5

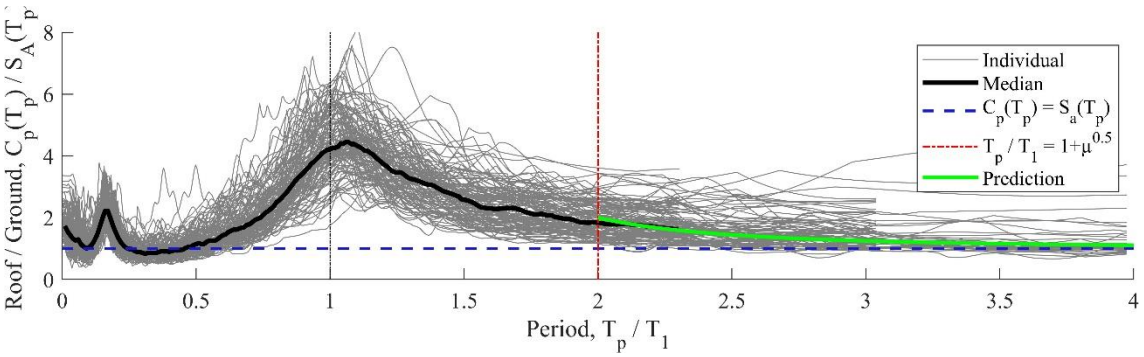

(b) Structural ductility μ = 1.0

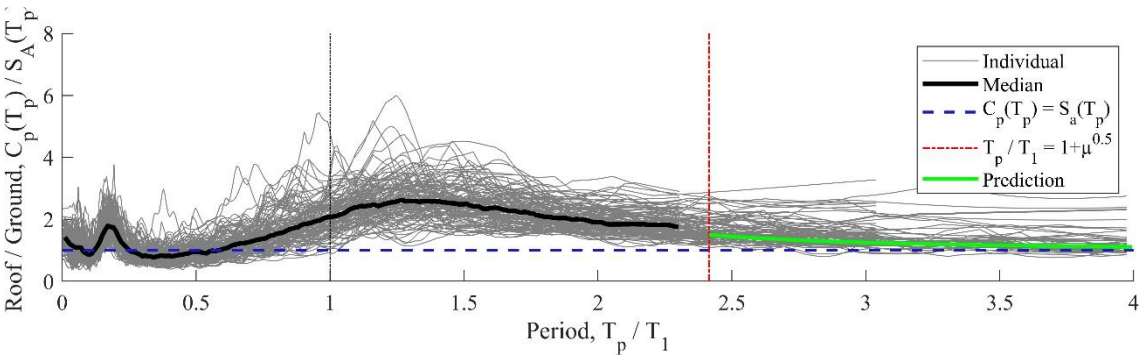

(c) Structural ductility μ = 2.0

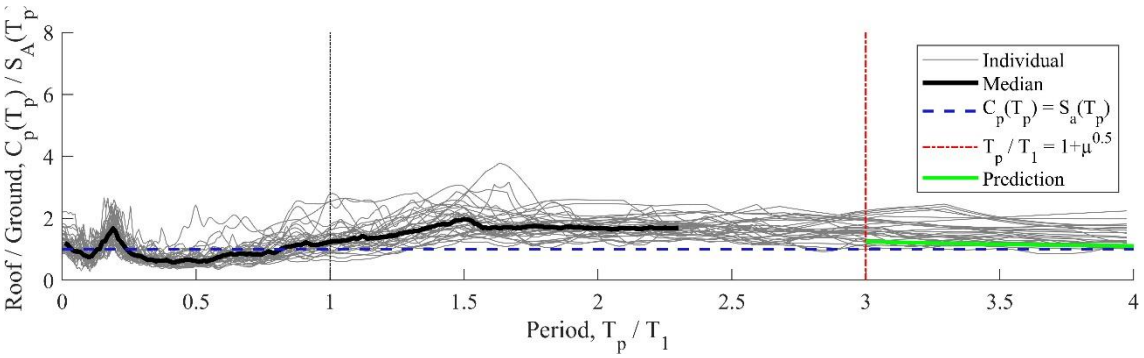

(d) Structural ductility μ = 4.0

Figure 6.7: Ratio of the roof to ground spectral accelerations computed using time history analysis of 4- 8- and 12-storey reinforced concrete wall buildings by Welch and Sullivan (2017), corresponding to four structural ductilities. Recommended provisions for long period parts and components are indicated.

6.9 Torsional Structural Response and In-Plane Diaphragm Flexibility

The approach recommended in this report does not make explicit allowances for the effects of in-plane diaphragm flexibility or torsional modes of vibration of the structure supporting the part or component. The demands estimated at the location that the part or component is mounted are assumed to have a constant distribution horizontally.

Figure 6.8(a) shows results reported in Appendix B of the ATC (2018) report relative to diaphragm flexibility. Based on these observations, the ATC(2018) report points out that diaphragm flexibility could increase demands significantly but it was decided to not to make engineers allow for it, potentially because they did not see enough evidence that it needed to be accounted for. It is noted herein that the amplifications observed as similar to those expected for flexible parts according to the recommendations. Hence, it is considered that flexible diaphragms could be accounted for in the recommended framework by treating them as flexible parts and components without requiring further modifications. This would increase the demands of the diaphragm, and rigid components mounted to the diaphragm, by a factor of 4.0. This could be subsequently reduced if the floor is deemed ductile, however.

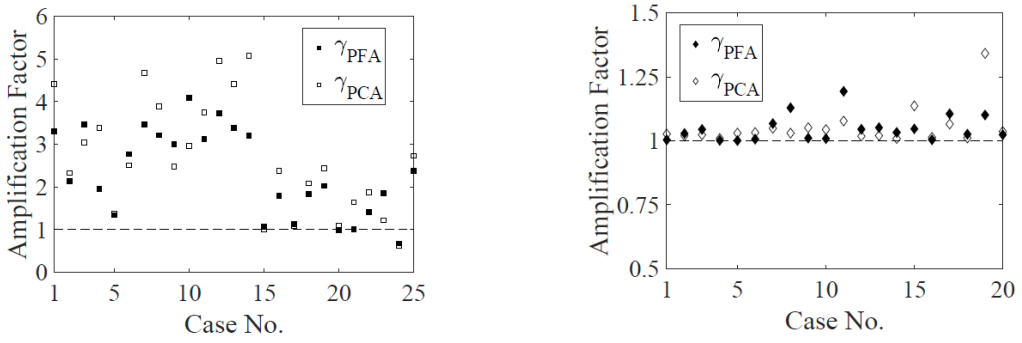

(a) in-plane diaphragm flexibility (sample size 25) ***(b) torsional building response (sample size 20)***

Figure 6.8: Amplified peak floor acceleration (PFA) and peak component acceleration (PCA) responses in the single-storey instrumented buildings due to in-plane diaphragm flexibility and torsional responses of supporting buildings. From the ATC-120 report (ATC, 2018).

Torsional modes of vibration may also contribute to the peak floor acceleration, as discussed in the ATC (2018) report. The approach developed by ATC (2018) considered this effect, contemplating an amplification factor, γ_{tor}, to account for the increase in floor acceleration at the perimeter as compared to the centre of rigidity. Figure 6.8(b) shows data evaluated by ATC (2018) for each direction of loading, comparing the peak value at a perimeter recording versus the average of the peak values of all the recordings on a floor. It was found that the increase in demand due to rotation of the floor and was on the order of approximately 1.2. It was noted, however, that peak values for each recording do not necessarily occur simultaneously. From this, the ATC (2018) report concluded that further research was required, and a torsional factor was not included in the nonstructural design equation. Further, it was

observed that the effects of torsion and in-plane diaphragm flexibility did not occur at the same time, suggesting that diaphragm flexibility may mitigate torsional effects. Kazantzi et al. (2018) recognised that torsional responses may result in dynamic amplifications for components with periods near the torsional modal periods of vibration that is similarly observed from translational structural modes. The recommended framework might therefore address this by using the flexible and rigid part response definitions but future research into torsional effects on buildings could investigate this further.

7 COMPARISON OF DESIGN LOADS ESTIMATED USING THE RECOMMENDED AND CURRENT APPROACHES

The impact of adopting the recommended approach for the estimation of the part horizontal design force is examined here using illustrative applications. For this, four case studies are conceived, consisting of one-, four-, six-, and twenty-storey buildings in Christchurch and Wellington. The fundamental period was estimated using the simplified approach given in the NZS1170.5 commentary, given in Equation 7.1:

$$T_1 = 1.25\, k_t h_n{}^{0.75} \tag{7.1}$$

The k_t value of 0.075 for concrete moment resisting frames was used. The storey height was taken as a constant 3.75 m. The fundamental periods were subsequently computed as 0.253 s, 0.715 s, 0.969 s, and 2.389 s for the 1-, 4-, 6-, and 20-storey buildings, respectively. Loads were specified for Class D (NZS1170.5) site class, also referred to here as a Class IV site, assuming a moderately stiff soil with $V_{s,30}$ between 250m/s and 300m/s. Design return periods of 25, 500, and 2500 years were considered. The assumed intensity of design ground shaking for these return periods was computed both for the existing NZS1170.5 loads and a representation of the updated New Zealand seismic hazard model (https://nshm.gns.cri.nz/), referred to as NZSHM (and later in this report as "NZHSM loading"). Consequently, the peak ground acceleration, *PGA*, and short period spectral accelerations, S_{AS}, (corresponding to the peak elastic spectral acceleration plateau for horizontal shaking in the short period range) adopted in this study are given in Table 7.1.

Table 7.1: The peak ground acceleration, *PGA*, and short period spectral accelerations, S_{AS}, from NZS1170.5 and 2022 update of New Zealand seismic hazard model (NZSHM) for three considered return periods.

	25 year			500 year			2500 year		
	NZS1170.5	NZSHM		NZS1170.5	NZSHM		NZS1170.5	NZSHM	
	PGA	*PGA*	S_{AS}	*PGA*	*PGA*	S_{AS}	*PGA*	*PGA*	S_{AS}
Christchurch	0.08 g	0.09 g	0.19 g	0.34 g	0.43 g	0.93 g	0.60 g	0.75 g	1.62 g
Wellington	0.11 g	0.16 g	0.35 g	0.45 g	0.86 g	1.70 g	0.81 g	1.49 g	2.93 g

The part horizontal design force were computed for part ductility values, μ_p, of 1.25 and 2.5, and structural ductility values, μ, of 1.0 and 4.0. The current NZS1170.5 approach was applied using both the existing NZS1170.5 and NZSHM loading, whereas the recommended method was applied considering only the NZSHM loading, but considers both rigid and flexible components. This allows the comparison of the change in demands with the different loadings, with and without changing the parts and component calculation approach.

Table 7.2 and 7.3 provide the part horizontal design force, F_{ph} / W_p, of flexible and rigid parts and components mounted at the roof level of the four case study buildings, computed for the hazard given for a 500 year return period on Class D / IV soil sites in Christchurch and Wellington.. These were computed using the NZSHM loading with the recommended and NZS1170.5 methods, and compared to the current NZS1170.5 design loads. The change in the part horizontal design force that would result from adopting the recommended method with the NZSHM loading is characterised considering the ratio of this value to the current NZS1170.5 approach and loadings, and the values computed if the NZS1170.5 approach is unchanged but NZSHM loading is adopted. This ratio is presented in the tables as percentages and denoted as prop/NZS, and is shown in red if values exceed 110% and shown in green if it is below 75%.

The part horizontal design force on rigid parts and components prescribed by the recommended method can be observed to be significantly lower than the current demands in most cases in Christchurch and Wellington. This effect is significantly more pronounced when the current approach is applied with the updated hazard. The perhaps counter-intuitively, the ratios of the values predicted by the recommended to current NZS1170.5 approaches are slightly greater for rigid parts for the ductile structure and part case, where μ is 4.0 and μ_p is 2.5, than the nominally elastic case, where μ is 1.0 and μ_p is 1.25. This is because the NZS1170.5 approach is applying a reduction for the ductility of the part, whereas it has been well established that rigid parts do not exhibit this behaviour. This reduction appears to be slightly greater than the structural nonlinearity reduction given by the recommended method. This same effect is present in the nominally-elastic-structure and ductile-part case, where μ is 1.0 and μ_p is 2.5, but the effects of structural nonlinearity are not as significant, as C_{str} adopts the lower bound value of 1.3 at the roof, and the ratio has consequently larger values.

The part horizontal design force on flexible parts and components prescribed by the recommended method is also lower than the current demands in most cases in Christchurch and, in some situations, Wellington. The demands on flexible parts using the current approach and loading increases by as much as a factor of two if the recommended method and updated hazard are adopted. This is predominantly due to the large increase in the seismic hazard for the Wellington region, as evidenced in the increase in the peak ground acceleration values shown in Table 7.1, that this is not as significant in the Christchurch case study applications, and that the ratio values significantly reduce when the current approach is applied with the NZSHM loading, despite the current approach capping some values at 3.6 g.

Single-storey structures are an exception to the recommended floor height coefficient formulation. There, the floor height coefficient is taken as the ratio of the short period spectral acceleration, S_{AS}, to the peak ground acceleration, *PGA*. This results in floor height coefficients of 2.2 and 2.0 for the 500 year hazard in Christchurch and Wellington, respectively. This is greater than the floor height coefficient computed using the current approach, which yields a value of 1.625 for a roof height of 3.75 m. This is why the single-storey structures exhibit larger ratios than the taller buildings. The use of the exception in the recommended approach removes the overly-conservative floor height coefficient of 3.5 that would otherwise result from using the approach from ASCE 7-22.

Table 7.2: Part horizontal design force, F_{ph} / W_p, of flexible and rigid parts and components mounted at the roof of the four case study buildings. This computed using the NZSHM loading with the recommended and NZS1170.5 methods. The current NZS1170.5 design loads are computed. Loading corresponds to a 500 year return period for a Class D / IV soil site in Christchurch.

		Flexible Parts and Components					Rigid Parts and Components				
		Proposed method	NZS1170.5 method		NZS1170.5 method		Proposed method	NZS1170.5 method		NZS1170.5 method	
		NZSHM	*NZS1170.5 hazard*	*prop/NZS*	*NZSHM*	*prop/NZS*	*NZSHM*	*NZS1170.5 hazard*	*prop/NZS*	*NZSHM*	*prop/NZS*
1 Storey	μ = 1 μ_p = 1.25	1.363 g	0.939 g	**145%**	1.188 g	**115%**	0.477 g	0.939 g	51%	1.188 g	40%
	μ = 1 μ_p = 2.5	0.477 g	0.553 g	86%	0.699 g	68%	0.477 g	0.553 g	86%	0.699 g	68%
	μ = 4 μ_p = 1.25	0.886 g	0.939 g	94%	1.188 g	75%	0.310 g	0.939 g	33%	1.188 g	26%
	μ = 4 μ_p = 2.5	0.310 g	0.553 g	56%	0.699 g	44%	0.310 g	0.553 g	56%	0.699 g	44%
4 Storey	μ = 1 μ_p = 1.25	1.944 g	1.734 g	**112%**	2.193 g	89%	0.680 g	1.734 g	39%	2.193 g	31%
	μ = 1 μ_p = 2.5	0.680 g	1.020 g	67%	1.290 g	53%	0.680 g	1.020 g	67%	1.290 g	53%
	μ = 4 μ_p = 1.25	1.264 g	1.734 g	73%	2.193 g	58%	0.442 g	1.734 g	26%	2.193 g	20%
	μ = 4 μ_p = 2.5	0.442 g	1.020 g	43%	1.290 g	34%	0.442 g	1.020 g	43%	1.290 g	34%
6 Storey	μ = 1 μ_p = 1.25	1.803 g	1.734 g	104%	2.193 g	82%	0.631 g	1.734 g	36%	2.193 g	29%
	μ = 1 μ_p = 2.5	0.631 g	1.020 g	62%	1.290 g	49%	0.631 g	1.020 g	62%	1.290 g	49%
	μ = 4 μ_p = 1.25	1.172 g	1.734 g	68%	2.193 g	53%	0.410 g	1.734 g	24%	2.193 g	19%
	μ = 4 μ_p = 2.5	0.410 g	1.020 g	40%	1.290 g	32%	0.410 g	1.020 g	40%	1.290 g	32%
20 Storey	μ = 1 μ_p = 1.25	1.506 g	1.734 g	87%	2.193 g	69%	0.527 g	1.734 g	30%	2.193 g	24%
	μ = 1 μ_p = 2.5	0.527 g	1.020 g	52%	1.290 g	41%	0.527 g	1.020 g	52%	1.290 g	41%
	μ = 4 μ_p = 1.25	0.979 g	1.734 g	56%	2.193 g	45%	0.343 g	1.734 g	20%	2.193 g	16%
	μ = 4 μ_p = 2.5	0.343 g	1.020 g	34%	1.290 g	27%	0.343 g	1.020 g	34%	1.290 g	27%

Table 7.3: Part horizontal design force, F_{ph} / W_p, of flexible and rigid parts and components mounted at the roof of the four case study buildings. This computed using the NZSHM loading with the recommended and NZS1170.5 methods. The current NZS1170.5 design loads are computed. Loading corresponds to a 500 year return period for a Class D / IV soil site in Wellington.

		Flexible Parts and Components					Rigid Parts and Components				
		Proposed method	NZS1170.5 method		NZS1170.5 method		Proposed method	NZS1170.5 method		NZS1170.5 method	
		NZSHM	*NZS1170.5 hazard*	*prop/NZS*	*NZSHM*	*prop/NZS*	*NZSHM*	*NZS1170.5 hazard*	*prop/NZS*	*NZSHM*	*prop/NZS*
1 Storey	μ = 1 μ_p = 1.25	2.491 g	1.243 g	**200%**	2.376 g	105%	0.872	1.243 g	70%	2.376 g	37%
	μ = 1 μ_p = 2.5	0.872 g	0.731 g	**119%**	1.398 g	62%	0.872	0.731 g	**119%**	1.398 g	62%
	μ = 4 μ_p = 1.25	1.619 g	1.243 g	**130%**	2.376 g	68%	0.567	1.243 g	46%	2.376 g	24%
	μ = 4 μ_p = 2.5	0.567 g	0.731 g	77%	1.398 g	41%	0.567	0.731 g	77%	1.398 g	41%
4 Storey	μ = 1 μ_p = 1.25	3.888 g	2.295 g	**169%**	3.600 g	108%	1.361	2.295 g	59%	3.600 g	38%
	μ = 1 μ_p = 2.5	1.361 g	1.350 g	101%	2.580 g	53%	1.361	1.350 g	101%	2.580 g	53%
	μ = 4 μ_p = 1.25	2.527 g	2.295 g	**110%**	3.600 g	70%	0.885	2.295 g	39%	3.600 g	25%
	μ = 4 μ_p = 2.5	0.885 g	1.350 g	66%	2.580 g	34%	0.885	1.350 g	66%	2.580 g	34%
6 Storey	μ = 1 μ_p = 1.25	3.606 g	2.295 g	**157%**	3.600 g	100%	1.262	2.295 g	55%	3.600 g	35%
	μ = 1 μ_p = 2.5	1.262 g	1.350 g	93%	2.580 g	49%	1.262	1.350 g	93%	2.580 g	49%
	μ = 4 μ_p = 1.25	2.344 g	2.295 g	102%	3.600 g	65%	0.820	2.295 g	36%	3.600 g	23%
	μ = 4 μ_p = 2.5	0.820 g	1.350 g	61%	2.580 g	32%	0.820	1.350 g	61%	2.580 g	32%
20 Storey	μ = 1 μ_p = 1.25	3.012 g	2.295 g	**131%**	3.600 g	84%	1.054	2.295 g	46%	3.600 g	29%
	μ = 1 μ_p = 2.5	1.054 g	1.350 g	78%	2.580 g	41%	1.054	1.350 g	78%	2.580 g	41%
	μ = 4 μ_p = 1.25	1.958 g	2.295 g	85%	3.600 g	54%	0.685	2.295 g	30%	3.600 g	19%
	μ = 4 μ_p = 2.5	0.685 g	1.350 g	51%	2.580 g	27%	0.685	1.350 g	51%	2.580 g	27%

The design loads given by the current and recommended approaches provisions are demonstrated visually in Figure 7.1, which shows the part horizontal design force, F_{ph} / W_p, of flexible and rigid parts and components mounted throughout a twenty-storey building in Wellington for a 500 year return period. This computed using the NZSHM loading with the recommended and NZS1170.5 methods, and compared with the current NZS1170.5 design loads.

The horizontal design forces for rigid parts and components computed using the recommended method are below the current design loads and current approach at all floors, and is only slightly greater at the ground level for the high part ductility case in Figure 7.1(b). The design force for flexible parts computed using the recommended approach, however, exceeds the current design force at the ground level, the first and second floors, regardless of structural ductility, and the upper three floors where the structural ductility value is 1.0. The development of part ductility of 2.5 or greater in flexible parts is able to reduce the amplification given by the spectral shape factor to provide the same design loads as rigid components, as the ratio of the spectral shape factor and horizontal part response factor, [$Ci(T_p)$ / C_{ph}], is is [4.0/4.0] for flexible parts and [1.0/1.0] for rigid parts, as shown in Figure 7.1(b).

The development of structural nonlinearity is able to significantly reduce the demands at the roof, and the effect is less pronounced with decreasing relative floor height. The horizontal design forces over the mid-height of the building are significantly lower than the current design loads, however, which have been widely observed to be overly conservative. The values estimated using the recommended approach is consistently below those computed with the current NZS1170.5 approach using the same NZSHM loading.

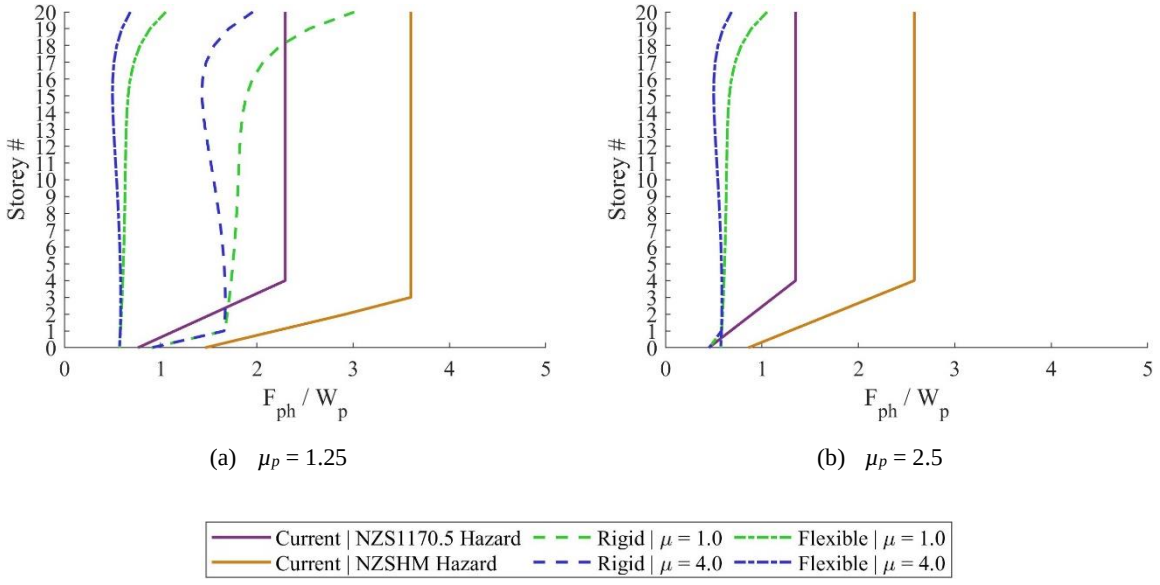

Figure 7.1: Part horizontal design force, F_{ph} / W_p, of flexible and rigid parts and components in Wellington for a twenty-storey building. This computed using the NZSHM loading with the recommended and NZS1170.5 methods. The current NZS1170.5 design loads are computed. Loading corresponds to a 500 year return period for a Class D / IV soil site.

NZS1170.5 states that parts supported directly on the ground floor are to be designed as a separate structure with design actions derived using Section 5 of the standard, with characteristics determined in Section 4. Here, however, the forces are computed using the provisions in Section 8, considering a floor height, h_i, of 0. The recommended approach can be observed to result in significantly lower demands than the application of the current approach with the NZSHM loading, and similar forces to those computed using the current approach with current loading.

Figures 7.2 to 7.9 show the computed values for the part horizontal design force normalised by the weight of the part with a distribution with height. Figures 7.2 to 7.5 correspond to the Christchurch hazard, whereas Figures 7.6 to 7.9 are for Wellington. The figures are shown for the 1-, 4-, 6-, and 20-storey buildings consecutively.

Christchurch almost never exceeds current hazard and current code approach. The peak ground accelerations prescribed in NZSHM is not significantly greater than those from NZS1170.5. as shown in Table 7.1. The Wellington hazard has significantly increased, however, and the forces at some levels exceed the application of the current approach. The apparently arbitrary 3.6 g cap on the design force in the current NZS1170.5 is often reached where the NZSHM hazard is considered, and thus the recommended approach results in larger design values.

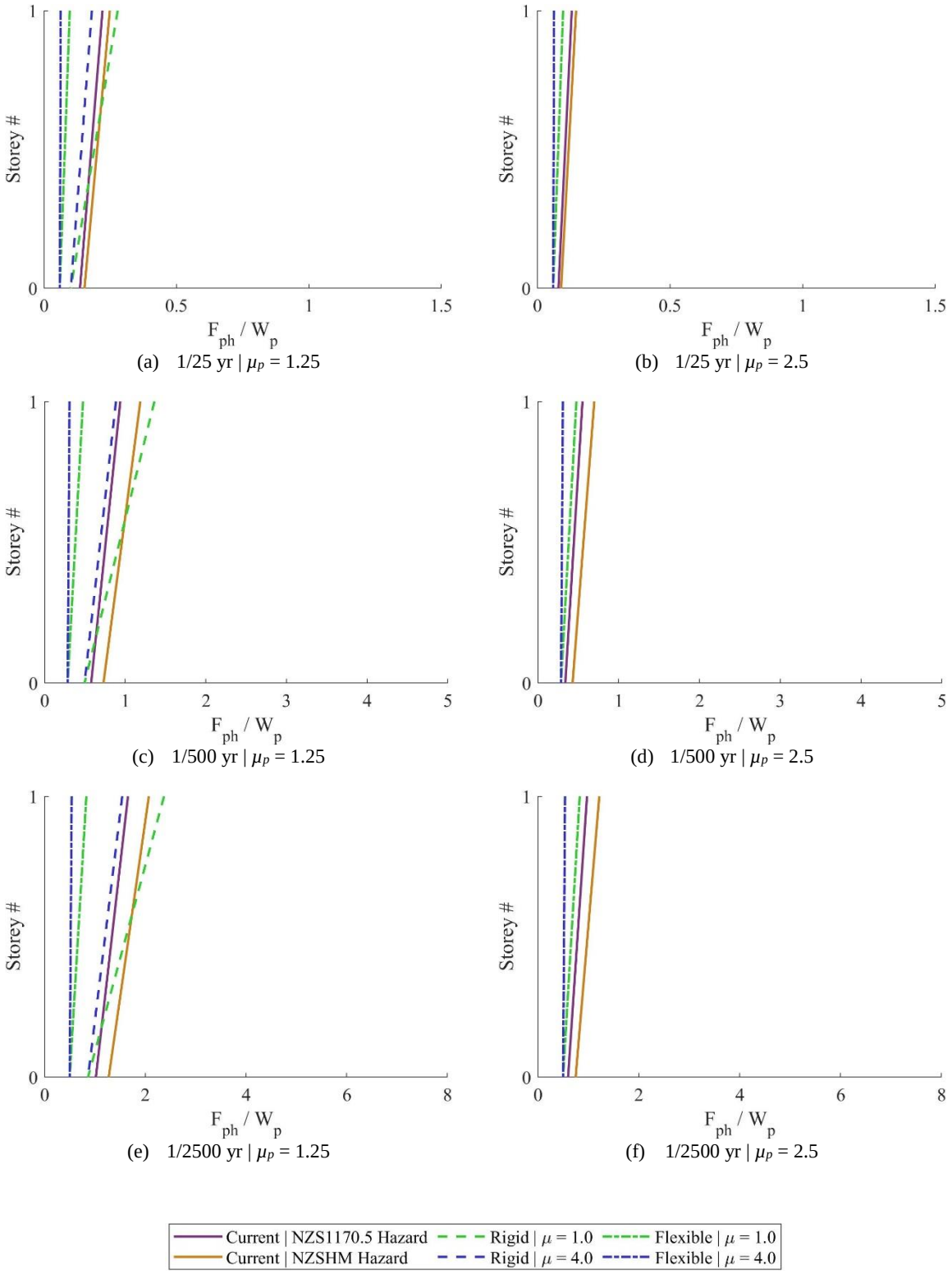

Figure 7.2: Part horizontal design force, F_{ph} / W_p, of flexible and rigid parts and components in Christchurch for a one-storey building. This computed using the NZSHM loading with the recommended and NZS1170.5 methods. The current NZS1170.5 design loads are computed.

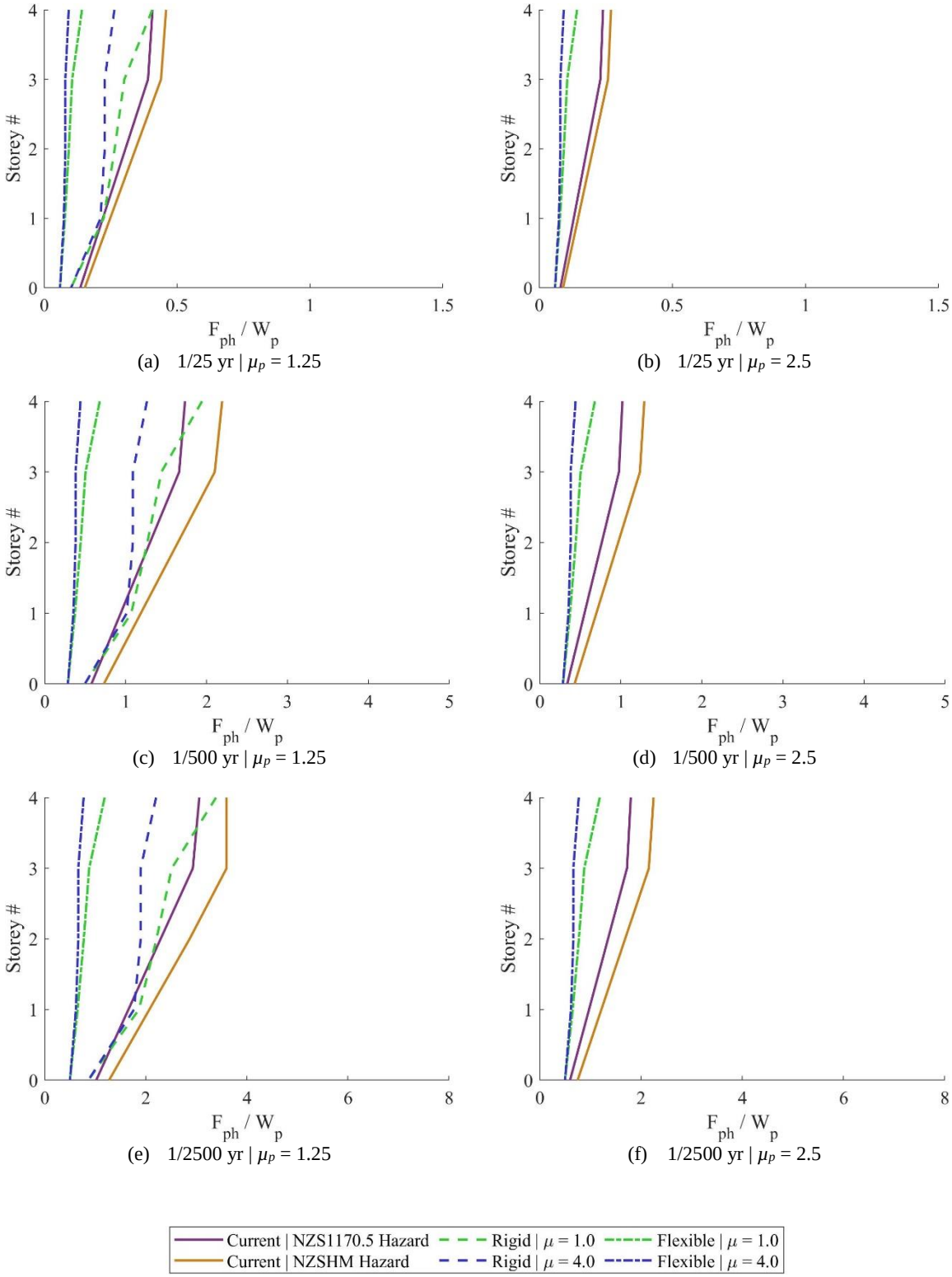

Figure 7.3: Part horizontal design force, F_{ph} / W_p, of flexible and rigid parts and components in Christchurch for a four-storey building. This computed using the NZSHM loading with the recommended and NZS1170.5 methods. The current NZS1170.5 design loads are computed.

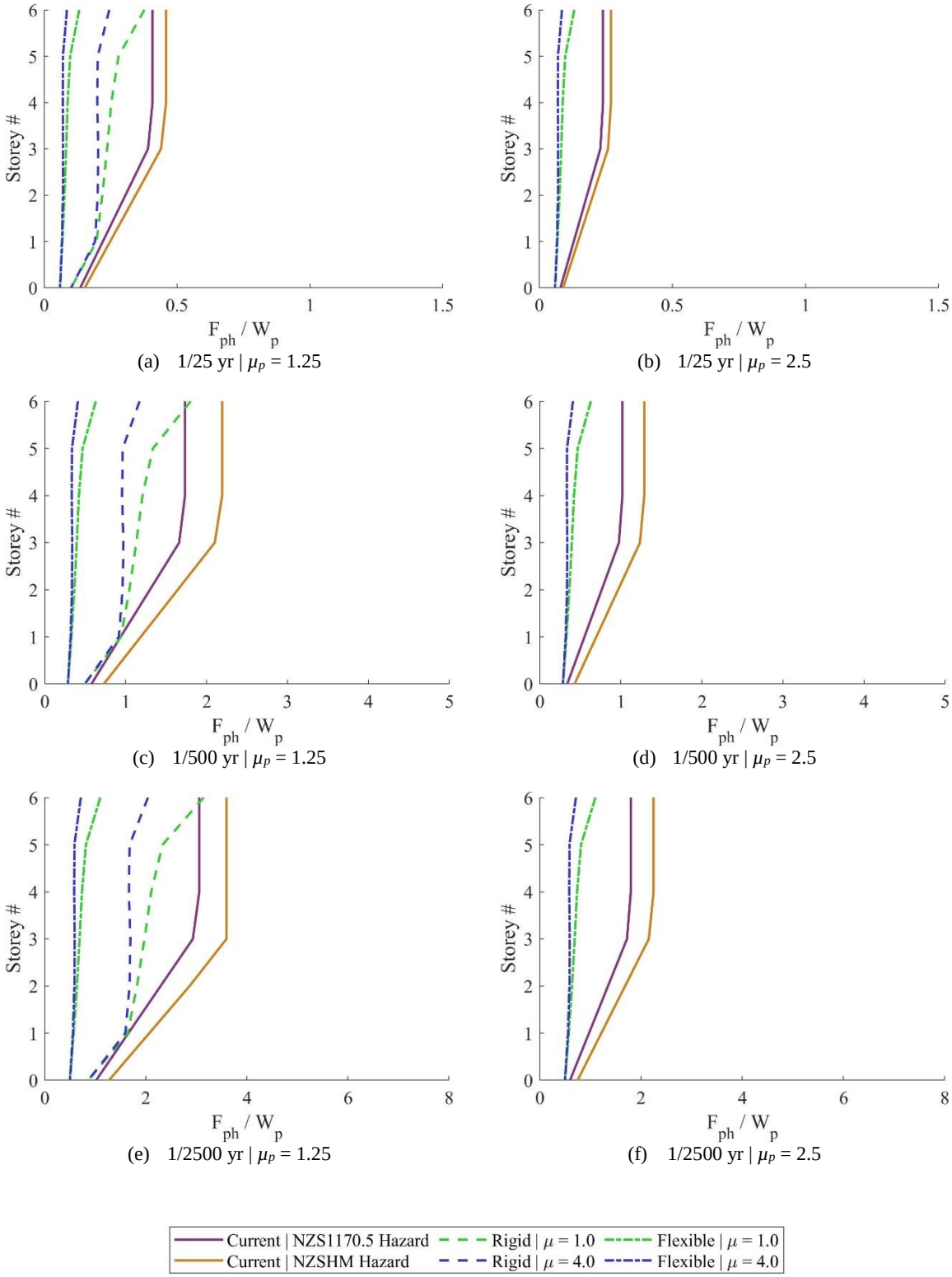

Figure 7.4: Part horizontal design force, F_{ph} / W_p, of flexible and rigid parts and components in Christchurch for a six-storey building. This computed using the NZSHM loading with the recommended and NZS1170.5 methods. The current NZS1170.5 design loads are computed.

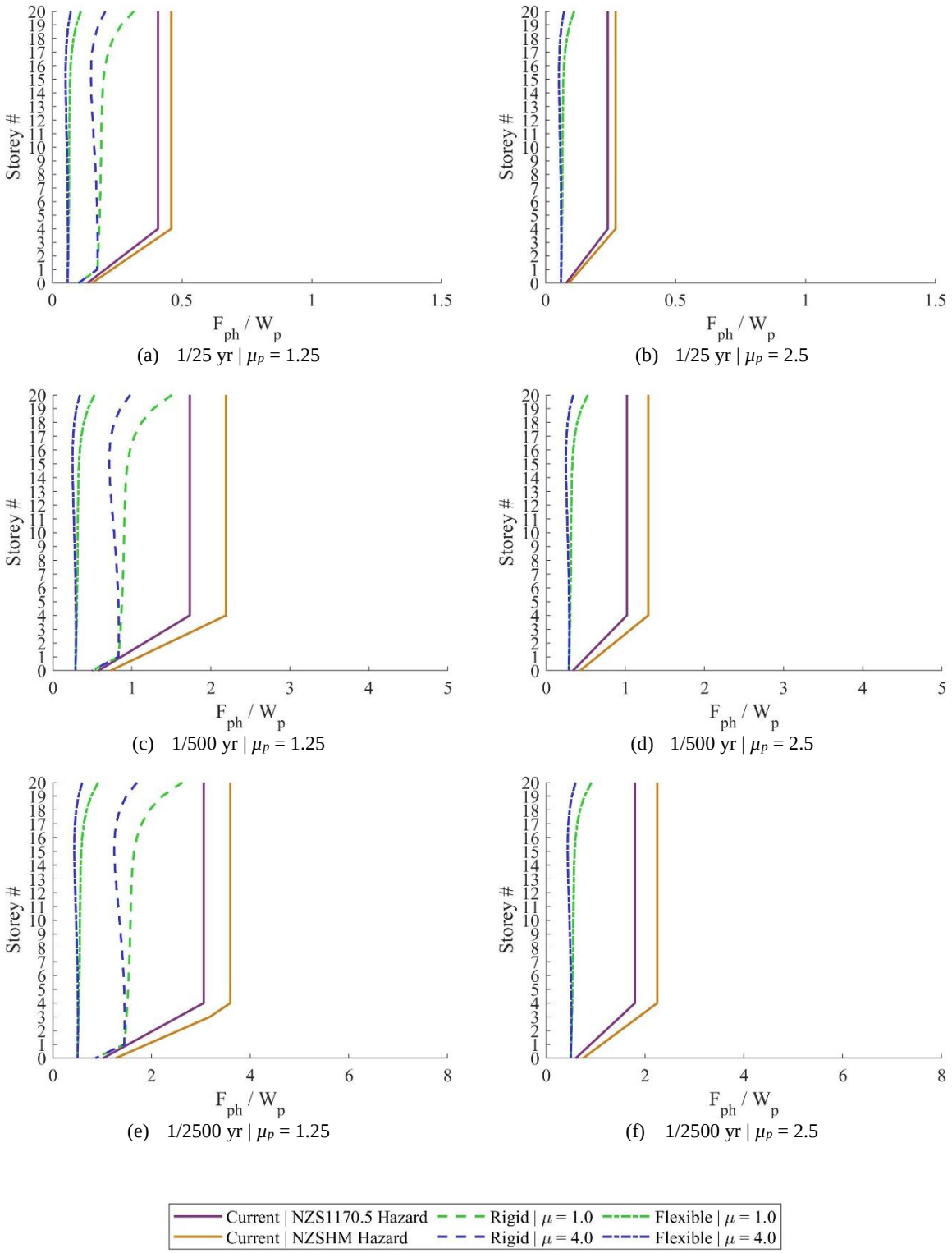

Figure 7.5: Part horizontal design force, F_{ph} / W_p, of flexible and rigid parts and components in Christchurch for a twenty-storey building. This computed using the NZSHM loading with the recommended and NZS1170.5 methods. The current NZS1170.5 design loads are computed.

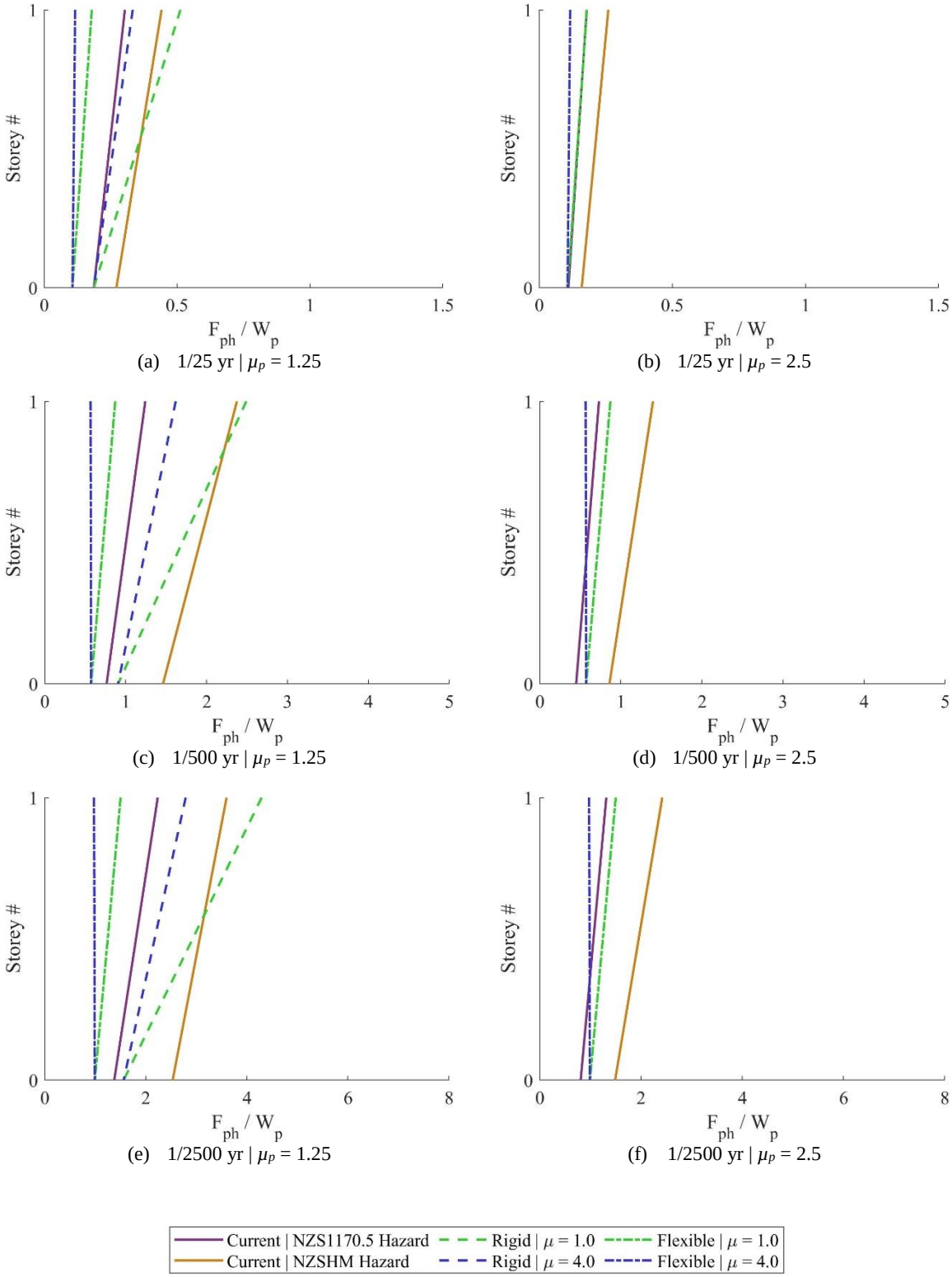

Figure 7.6: Part horizontal design force, F_{ph} / W_p, of flexible and rigid parts and components in Wellington for a one-storey building. This computed using the NZSHM loading with the recommended and NZS1170.5 methods. The current NZS1170.5 design loads are computed.

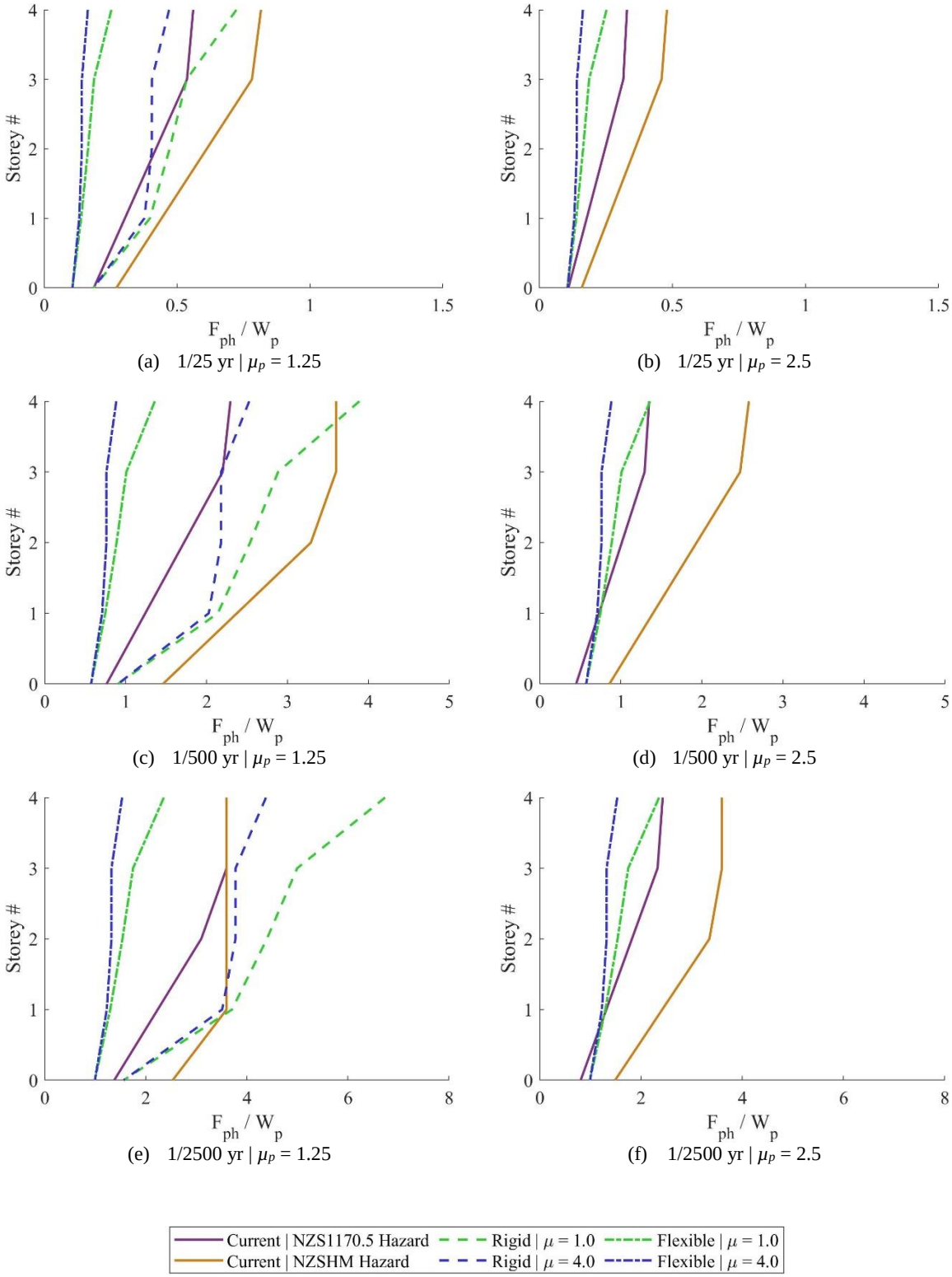

Figure 7.7: Part horizontal design force, F_{ph} / W_p, of flexible and rigid parts and components in Wellington for a four-storey building. This computed using the NZSHM loading with the recommended and NZS1170.5 methods. The current NZS1170.5 design loads are computed.

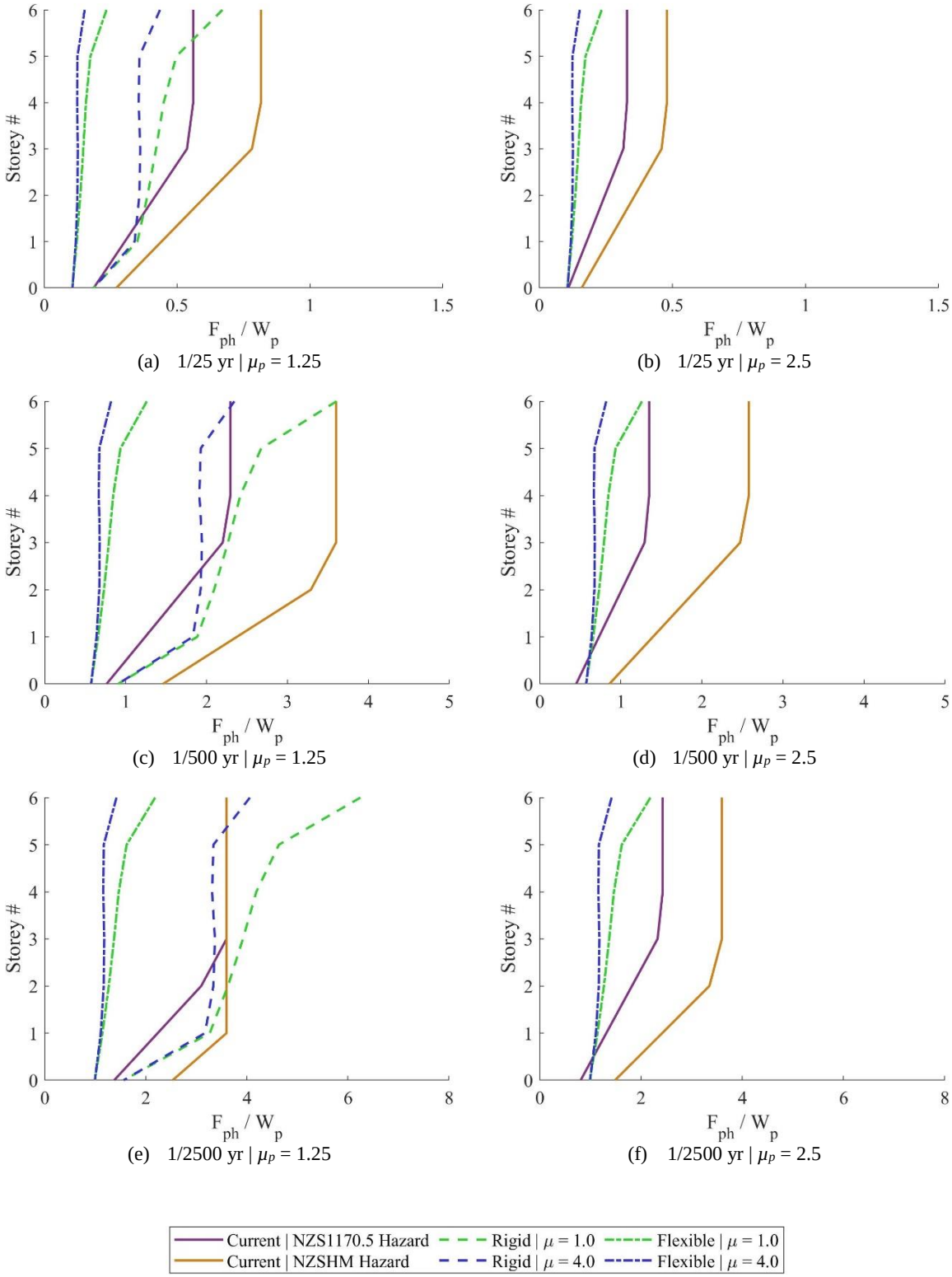

Figure 7.8: Part horizontal design force, F_{ph} / W_p, of flexible and rigid parts and components in Wellington for a six-storey building. This computed using the NZSHM loading with the recommended and NZS1170.5 methods. The current NZS1170.5 design loads are computed.

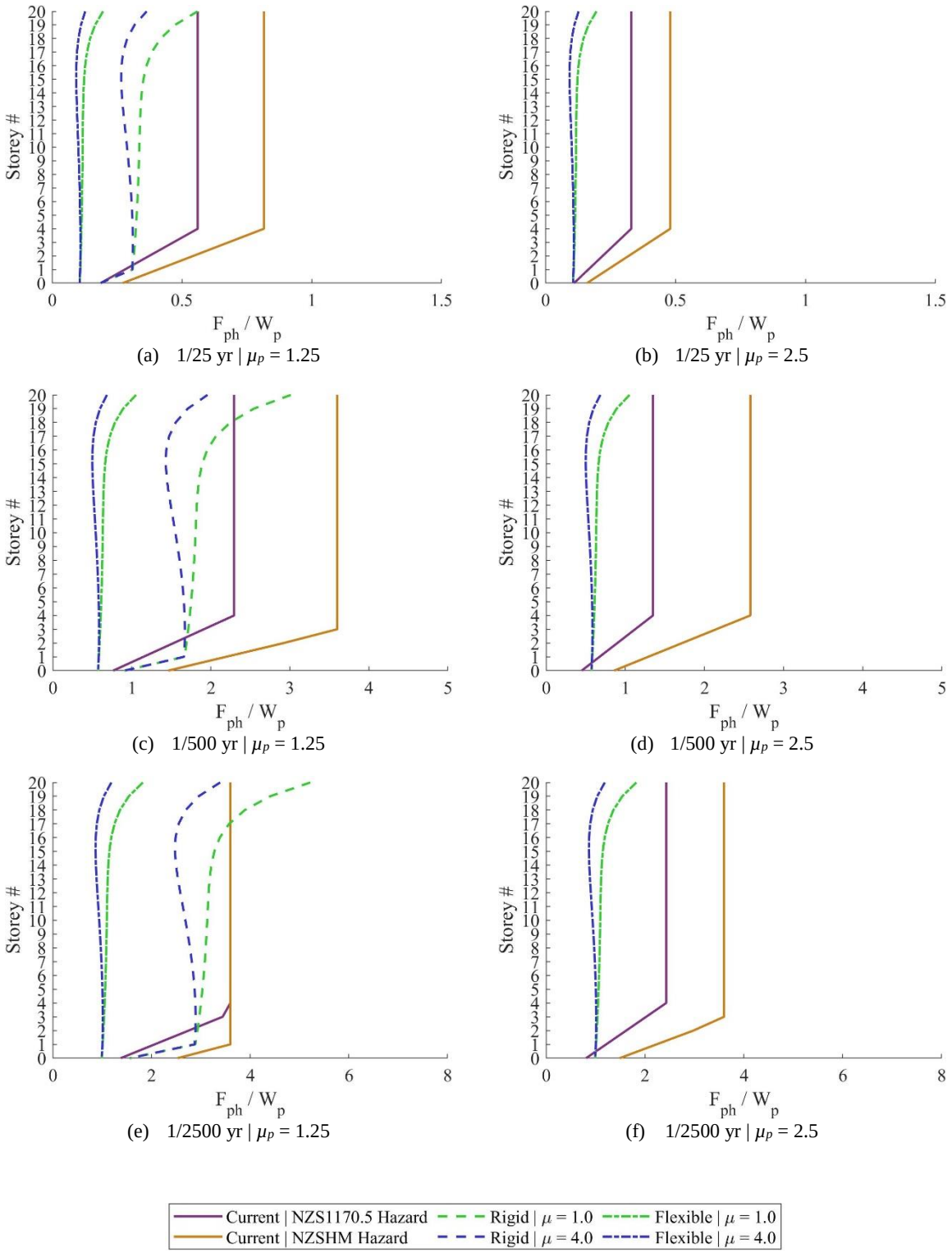

Figure 7.9: Part horizontal design force, F_{ph} / W_p, of flexible and rigid parts and components in Wellington for a twenty-storey building. This computed using the NZSHM loading with the recommended and NZS1170.5 methods. The current NZS1170.5 design loads are computed.

A 2016 amendment to NZS1170.5 states that for serviceability limit state one, SLS1, associated with a return period of 25 years, the ductility of the part, μ_p, shall not be taken greater than 1.0, unless otherwise determined by special study but in no circumstances shall be taken greater than or equal to 1.25. Consequently, the demands described for the 25 year hazard in (a) and (b) of Figures 7.2 to 7.9 do not adequately illustrate the current application of the standard. Instead, design is conducted considering the elastic structure and elastic part, where μ and μ_p are equal to 1.0. Figures 7.10 and 7.11 show the part horizontal design force, F_{ph} / W_p, of elastic flexible and rigid parts and components for the four case study buildings considering an SLS1 25 year return period hazard in Christchurch and Wellington, respectively. The forces were computed through the application of the recommended method with NZSHM loads and the current NZS1170.5 approach using the old and new loadings.

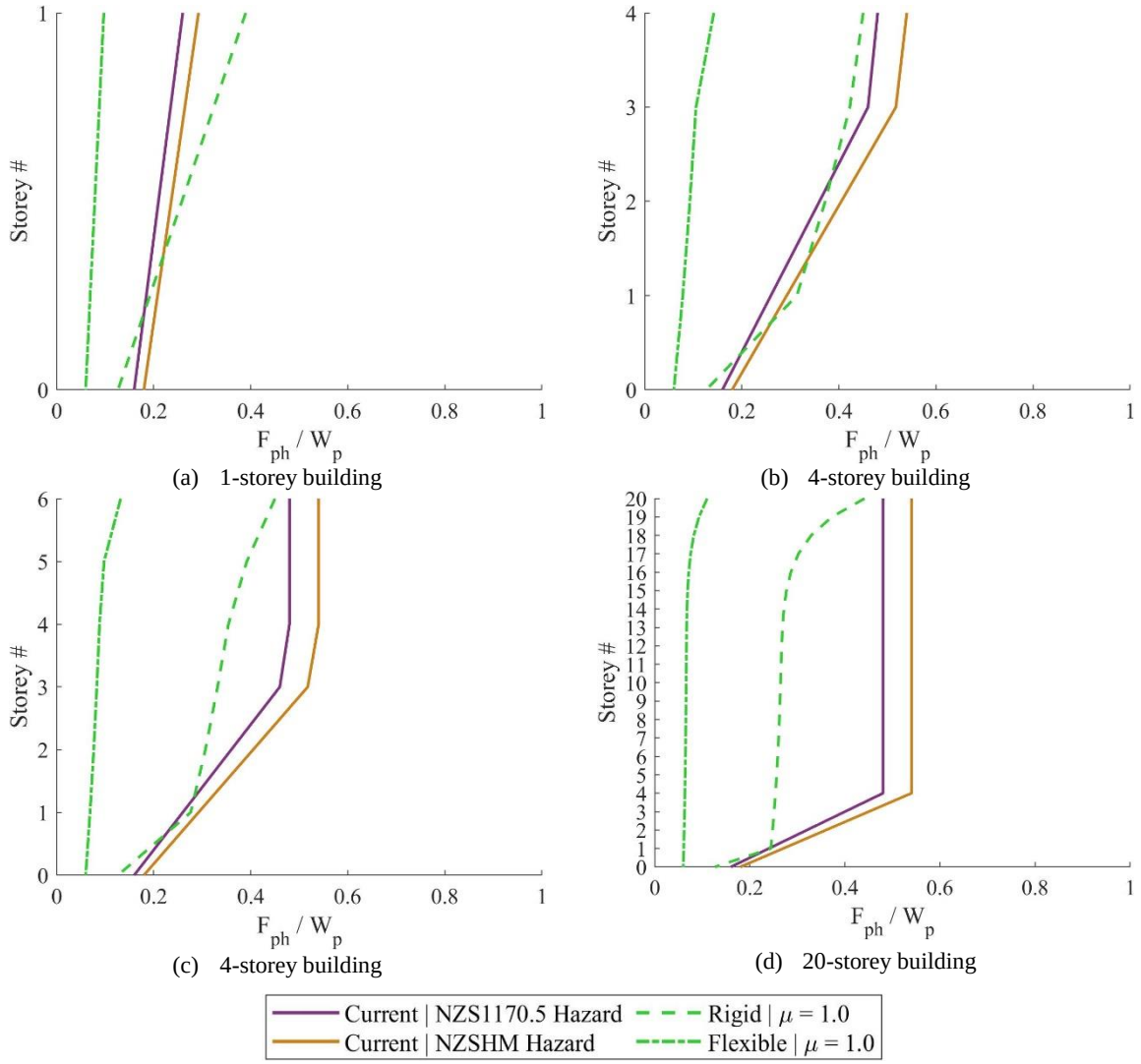

Figure 7.10: Part horizontal design force, F_{ph} / W_p, of flexible and rigid parts and components considering an SLS1 25 year return period hazard in Christchurch for the four case study buildings. This computed using the NZSHM loading with the recommended and NZS1170.5 methods. The current NZS1170.5 design loads are computed.

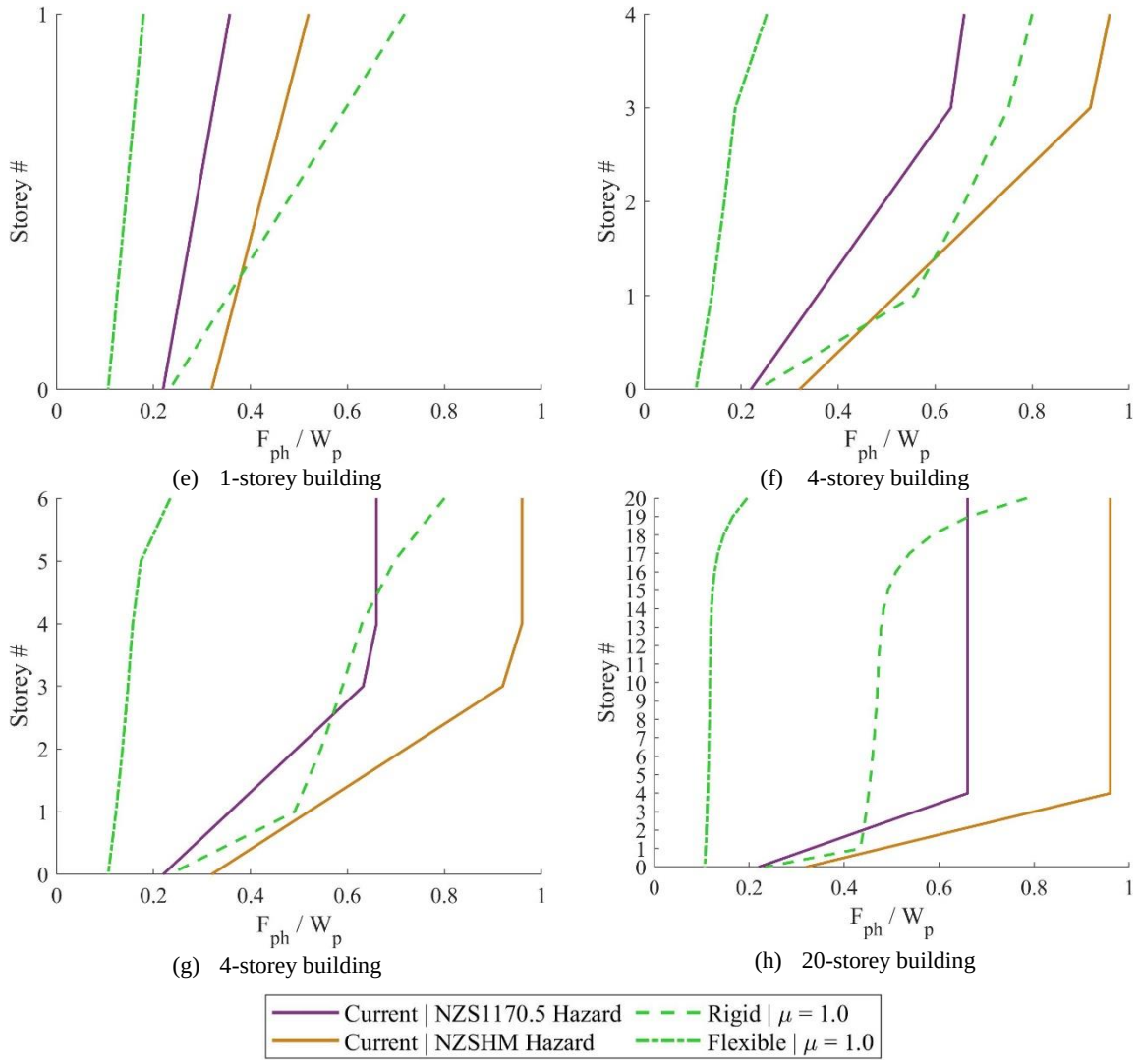

Figure 7.11: Part horizontal design force, F_{ph} / W_p, of flexible and rigid parts and components considering an SLS1 25 year return period hazard in Wellington for the four case study buildings. This computed using the NZSHM loading with the recommended and NZS1170.5 methods. The current NZS1170.5 design loads are computed.

The part horizontal design forces for rigid parts and components is once more significantly lower in all applications when computed using the recommended method than the current NZS1170.5 approach. The design force for flexible parts and components estimated using the recommended approach is lower than the corresponding applications of the current NZS1170.5 approach for the Christchurch loading at all floors, excluding the first floor. A similar pattern is observed in the application of the approaches with the Wellington loading, although the demands at the roof level can be observed to be greater using the recommended approach.

There is a distinct discontinuity between the part horizontal design forces for flexible components mounted at the ground and first floor levels. This is due to the definition of the spectral shape factor, $Ci(T_p)$, which adopts a value of 4.0 for flexible parts mounted above the ground level, and adopts the

ratio of the short period ground spectral acceleration, S_{AS}, and the peak ground acceleration, *PGA*, for components mounted at or below the ground level, as this is the greatest amplification that is expected to develop at the ground level. The application of the recommended method shown in Figures 7.10 and 7.11 use the spectral shape factor values of 2.1 and 2.2 for Christchurch and Wellington, respectively. This discontinuity is not representative of the true spectral amplification observed, as the spectral accelerations of parts mounted over the lowest levels of the structure are not significantly altered by dynamic amplification induced by the modal response of the structure. Instead, floor acceleration response spectra over the lowest levels of the structure exhibit only minor amplification above the corresponding ground acceleration response spectra. The basis of the spectral shape factors were recommended here for simplicity of adoption, and is conservative over these lower levels. The discontinuity can be effectively reduced through the development of ductility of the part, as demonstrated in Figures 7.2 to 7.9 where the part ductility values of 1.25 and 2.5 are used.

8 CONCLUSIONS

This report examined the current state of practice for the design for seismic loading of parts and components within buildings in New Zealand and the provisions recently developed by the Applied Technology Council subsequently adopted in ASCE 7-22. The findings of the research suggest that revisions should be made to *Section 8 Requirements for Parts and Components* of the New Zealand Standard *NZS 1170.5:2004 Structural Design Actions, Part 5: Earthquake Actions*. Updates to the parts and components approach were recommended, benefitting from insight provided through the recent ASCE 7-22 procedure and research in the literature. To gauge the performance of the parts and components approach with updates, comparisons were made with data from instrumented buildings and numerical models.

The recommended revisions were trialled using loading representative of the 2022 New Zealand seismic hazard model results. The results were compared with those obtained through application of the current NZS 1170.5 parts and components approach and hazard, as well as the current NZS 1170.5 parts and components approach with the updated national seismic hazard. The results suggest that demands on parts that are expected to be resonant with the building period and that are characterised by low ductility capacity would be expected to attract larger design loads. However, for most parts, the results indicate that substantial reductions in design loading may be achieved using the updated approach, particularly for parts and components that are rigid, develop nonlinear response, or are mounted over the lower levels of the structure.

9 REFERENCES

American Society of Civil Engineers. (2017). *ASCE/SEI 7-16: Minimum design loads and associated criteria for buildings and other structures*.

American Society of Civil Engineers. (2021). *ASCE/SEI 7-22 Minimum Design Loads and Associated Criteria for Buildings and Other Structures*.

Applied Technology Council. (2018). *Recommendations for improved seismic performance of nonstructural components*. https://doi.org/10.6028/NIST.GCR.18-917-43

Aragaw, L. F. (2017). *Floor Response Spectra in Hybrid Base-Rocking and Reinforced Concrete Wall Buildings*. University of Washington.

Biggs, J. M. (1971). Seismic response spectra for equipment design in nuclear power plants. *First International Conference on "Structural Mechanics in Reactor Technology,"* 329–343.

Buccella, N. (2019). *Nonstructural components in controlled rocking braced frames*. McMaster University.

Buccella, N., Wiebe, L., Konstantinidis, D., & Steele, T. (2021). Demands on nonstructural components in buildings with controlled rocking braced frames. *Earthquake Engineering & Structural Dynamics*, *50*(4), 1063–1082. https://doi.org/10.1002/eqe.3385

Calvi, P. M. (2014). Relative Displacement Floor Spectra for Seismic Design of Non Structural Elements. *Journal of Earthquake Engineering*, *18*(7), 1037–1059. https://doi.org/10.1080/13632469.2014.923795

Calvi, P. M., & Ruggiero, D. M. (2017). Earthquake-induced floor accelerations in base isolated structures. *16th World Conference on Earthquake Engineering*.

Carr, A.J. (2006). *RUAUMOKO3D-Inelastic dynamic analysis program*.

Carr, Athol J. (2016). *INSPECT In-elastic Response Spectra Computation*. Carr Research Ltd.

Chandramohan, R., Ma, Q., Wotherspoon, L. M., Bradley, B. A., Nayyerloo, M., Uma, S. R., & Stephens, M. T. (2017). Response of instrumented buildings under the 2016 Kaikoura earthquake. *Bulletin of the New Zealand Society for Earthquake Engineering*, *50*(2), 237–252. https://doi.org/10.5459/bnzsee.50.2.237-252

Dhakal, R. P., Pourali, A., Tasligedik, A. S., Yeow, T., Baird, A., MacRae, G., Pampanin, S., & Palermo, A. (2016). Seismic performance of non-structural components and contents in buildings: an overview of NZ research. *Earthquake Engineering and Engineering Vibration*, *15*(1), 1–17. https://doi.org/0.1007/s11803-016-0301-9

Drake, R. M., & Bachman, R. E. (1995). Interpretation of instrumented building seismic data and implications for building codes. *Structural Engineers Association of California Conference*.

European Committee for Standardization. (2004). *Eurocode 8: Design of structures for earthquake resistance - Part 1: General rules, seismic actions and rules for buildings*.

Fathali, S., & Lizundia, B. (2011). Evaluation of current seismic design equations for nonstructural components in tall buildings using strong motion records. *The Structural Design of Tall and Special Buildings*, *20*(S1), 30–46. https://doi.org/10.1002/tal.736

Federal Emergency Management Agency. (2012). *FEMA E-74: Reducing the Risks of Nonstructural*

Earthquake Damage – A Practical Guide.

Federal Emergency Management Agency (FEMA). (2009). *FEMA P695: Recommended Methodology for Quantification of Building System Performance and Response Parameters. Project ATC-63*.

Feinstein, T., & Moehle, J. P. (2022). Seismic response of floor-anchored nonstructural components fastened with yielding elements. *Earthquake Engineering & Structural Dynamics*, *51*(1), 3–21. https://doi.org/10.1002/eqe.3553

Filiatrault, A., & Sullivan, T. J. (2014). Performance-based seismic design of nonstructural building components: The next frontier of earthquake engineering. *Earthquake Engineering and Engineering Vibration*, *13*(S1), 17–46. https://doi.org/10.1007/s11803-014-0238-9

GeoNet. (2022). *Structural Array Data*. https://www.geonet.org.nz/data/types/structural_arrays

Haymes, K. (2022). *Developing Procedures for the Prediction of Floor Response Spectra*. University of Canterbury.

Haymes, K., Sullivan, T., & Chandramohan, R. (2020). A practice-oriented method for estimating elastic floor response spectra. *Bulletin of the New Zealand Society for Earthquake Engineering*, *53*(3), 116–136. https://doi.org/10.5459/bnzsee.53.3.116-136

Kazantzi, A. K., Miranda, E., & Vamvatsikos, D. (2020). Strength-reduction factors for the design of light nonstructural elements in buildings. *Earthquake Engineering & Structural Dynamics*, *49*(13), 1329–1343. https://doi.org/10.1002/eqe.3292

Kazantzi, A., Vamvatsikos, D., & Miranda, E. (2018). Effect of yielding on the seismic demands of nonstructural elements. *16th European Conference on Earthquake Engineering*.

Kehoe, B. E. (2014). Defining rigid vs. flexible nonstructural components. *Tenth U.S. National Conference on Earthquake Engineering*.

Kehoe, B. E., & Hachem, M. (2003, January 1). Procedures for Estimating Floor Accelerations. *ATC-29-2 Seminar on Seismic Design, Performance, and Retrofit of Nonstructural Components in Critical Facilities*.

Kelly, T. E. (1978). Floor response of yielding structures. *Bulletin of the New Zealand Society for Earthquake Engineering*, *11*(4), 255–272. https://doi.org/10.5459/bnzsee.11.4.255-272

Khakurel, S., Dhakal, R. P., Yeow, T. Z., & Saha, S. K. (2020). Performance group weighting factors for rapid seismic loss estimation of buildings of different usage. *Earthquake Spectra*, 875529301990131. https://doi.org/10.1177/8755293019901311

Maniatakis, C. A., Psycharis, I. N., & Spyrakos, C. C. (2013). Effect of higher modes on the seismic response and design of moment-resisting RC frame structures. *Engineering Structures*, *56*, 417–430. https://doi.org/10.1016/j.engstruct.2013.05.021

Marsantyo, R., Shimazu, T., & Araki, H. (2000). Dynamic response of nonstructural systems mounted on floors of buildings. *12th World Conference on Earthquake Engineering*.

McHattie, S. (2013). *Seismic Response of the UC Physics Building in the Canterbury Earthquakes*. University of Canterbury.

Merino, R. J., Perrone, D., & Filiatrault, A. (2020). Consistent floor response spectra for performance-based seismic design of nonstructural elements. *Earthquake Engineering & Structural Dynamics*, *49*(3), 261–284. https://doi.org/10.1002/eqe.3236

Miranda, E., & Taghavi, S. (2009). A Comprehensive Study of Floor Acceleration Demands in Multi-Story Buildings. *Improving the Seismic Performance of Existing Buildings and Other Structures*, 616–626. https://doi.org/10.1061/41084(364)57

Priestley, M. J. N., Calvi, G. M., & Kowalsky, M. J. (2007). *Direct displacement-based seismic design*. IUSS Press.

Rashid, M., Dhakal, R., & Sullivan, T. (2021). Seismic design of acceleration-sensitive non-structural elements in New Zealand: State-of-practice and recommended changes. *Bulletin of the New Zealand Society for Earthquake Engineering*, *54*(4), 243–262. https://doi.org/10.5459/bnzsee.54.4.243-262

Rodriguez, M. E., Restrepo, J. I., & Carr, A. J. (2002). Earthquake-induced floor horizontal accelerations in buildings. *Earthquake Engineering & Structural Dynamics*, *31*(3), 693–718. https://doi.org/10.1002/eqe.149

Ryu, K. P., Reinhorn, A. M., & Filiatrault, A. (2012). Full scale dynamic testing of large area suspended ceiling system. *15th World Conference on Earthquake Engineering*.

Shelton, R. H. (2004). Seismic response of building parts and and Non-Structural Components. In *Study Report, BRANZ Building of Knowledge*.

Standards New Zealand. (2016a). *NZS 1170.5:2004: Structural design actions, Part 5: Earthquake actions - New Zealand*.

Standards New Zealand. (2016b). *NZS 1170.5 Supp 1:2004 Structural design actions - Part 5: Earthquake actions - New Zealand Commentary*.

Sullivan, T. J., Calvi, P. M., & Nascimbene, R. (2013). Towards improved floor spectra estimates for seismic design. *Earthquakes and Structures*, *4*(1), 109–132. https://doi.org/10.12989/eas.2013.4.1.109

Tian, Y., Filiatrault, A., & Mosqueda, G. (2015). Seismic Response of Pressurized Fire Sprinkler Piping Systems I: Experimental Study. *Journal of Earthquake Engineering*, *19*(4), 649–673. https://doi.org/10.1080/13632469.2014.994147

Uma, S. R., Zhao, J. X., & King, A. B. (2010). Seismic actions on acceleration sensitive non-structural components in ductile frames. *Bulletin of the New Zealand Society for Earthquake Engineering*, *43*(2), 110–125. https://doi.org/10.5459/bnzsee.43.2.110-125

Villaverde, R. (1997). Seismic Design of Secondary Structures: State of the Art. *Journal of Structural Engineering*, *123*(8), 1011–1019. https://doi.org/10.1061/(ASCE)0733-9445(1997)123:8(1011)

Vukobratović, V., & Fajfar, P. (2017). Code-oriented floor acceleration spectra for building structures. *Bulletin of Earthquake Engineering*, *15*(7), 3013–3026. https://doi.org/10.1007/s10518-016-0076-4

Watkins, D., Chui, L., Hutchinson, T., & Hoehler, M. (2010). *Survey and Characterisation of Floor and Wall Mounted Mechanical and Electrical Equipment in Buildings. Report No. SSRP-2009/11*.

Welch, D. P. (2016). *Non-structural element considerations for contemporary performance-based earthquake engineering*. Scuola Universitaria Superiore IUSS Pavia.

Welch, D. P., & Sullivan, T. J. (2017). Illustrating a new possibility for the estimation of floor spectra in nonlinear multi-degree of freedom systems. *16th World Conference on Earthquake Engineering*.

APPENDIX A: CLASSIFICATION OF PARTS AND COMPONENTS FROM NZS1170.5 COMMENTARY AND ASCE/SEI7-22

Table A1: General classification of parts or components, expected ductility values at ultimate limit state (ULS) from ASCE 7-22.

Rigid parts or components	Rigid	-
Flexible parts or components		
High-deformability elements and attachments	Flexible	2.5
Limited-deformability elements and attachments	Flexible	1.5
Low-deformability materials and attachments	Flexible	1.25

Table A2: Suggested classification of architectural parts or components and expected ductility values at ULS.

Description of part or component	**Inferred Class from ASCE 7-22**	**Expected ductility at ULS**	
		ASCE 7-22	**NZS 1170.5**
Interior nonstructural walls and partitions			
Light frame ≤ 2.8 m in height	Rigid	-	3
Light frame > 2.8 m in height	Flexible	2.5	3
Reinforced masonry	Rigid	-	2
Glazed	Rigid	-	1
"All other walls and partitions"	Flexible	1.25	1.25
Cantilever elements (unbraced or braced to structural frame below its centre of mass)			
Parapets and cantilever interior nonstructural walls	Flexible	1.5	1.25
Chimneys where laterally braced or supported by the structural frame	Flexible	1.5	1.5
Cantilever elements (braced to structural frame above its centre of mass)			
Parapets	Rigid	-	1.25
Chimneys	Rigid	-	1.5
Exterior nonstructural walls	Rigid	-	2
Exterior nonstructural wall elements and connections			
Wall element	Rigid	-	2
Body of wall panel connections	Rigid	-	2
Structural glazing system	Rigid	-	1
Fasteners of the connecting system	Flexible	1.25	-
Veneer			
Limited-deformability elements and attachments	Rigid	-	2
Low-deformability elements and attachments	Rigid	-	

Description of part or component	Inferred Class from ASCE 7-22	Expected ductility at ULS	
		ASCE 7-22	NZS 1170.5
Penthouses (except where framed by an extension of the building frame)			
Seismic force-resisting systems with R ≥6	Flexible	2.5	
Seismic force-resisting systems with 4 ≤ R < 6	Flexible	1.5	
Seismic force-resisting systems with R < 4	Flexible	1.25	
Other systems	Flexible	1.25	
Ceilings			
All	Rigid	-	3
Cabinets			
Permanent floor-supported storage cabinets more than 1.8 m tall, including contents	Flexible	-	2
Permanent floor-supported library shelving, book stacks, and bookshelves more than 1.8 m tall, including contents	Flexible	-	3
Contents			
Laboratory equipment	Rigid	-	-
Computer access floor	Flexible	-	2
Process plant	Rigid	-	TBDD
Access floors	Flexible	1.25	3
Appendages and ornamentations	Flexible	1.5	1.25
Signs and billboards	Flexible	1.5	2
Egress stairways			
Egress stairways not part of the building seismic force-resisting system	Rigid	-	
Egress stairs and ramp fasteners and attachments	Flexible	1.5	
Concrete stairs	Flexible	-	2
Timber stairs	Flexible	-	3
Steel stairs	Flexible	-	4

NOTES:

1 TBDD means “To Be Determined by the Designer”.

2 External and internal walls are considered to be supported at top and bottom, otherwise they should be considered as canitlevers.

Table A3: Suggested classification of electrical parts or components and expected ductility values at ULS.

Description of part or component	Inferred Class from ASCE 7-22	Expected ductility at ULS	
		ASCE 7-22	NZS 1170.5
Air-side HVACR, fans, air handlers, air conditioning units, cabinet heaters, air distribution boxes, and other mechanical components constructed of sheet metal framing	Flexible	2.5	2 - 3
Wet-side HVACR, boilers, furnaces, atmospheric tanks and bins, chillers, water heaters, heat exchangers, evaporators, air separators, manufacturing or process equipment, and other mechanical components constructed of high-deformability materials	Rigid	-	1.25 - 2
Air coolers (fin fans), air-cooled heat exchangers, condensing units, dry coolers, remote radiators, and other mechanical components elevated on integral structural steel or sheet metal supports	Flexible	1.5	-
Engines, turbines, pumps, compressors, and pressure vessels not supported on skirts	Rigid	-	1.25
Skirt-supported pressure vessels	Flexible	1.5	2
Generators, batteries, inverters, motors, transformers, and other electrical components constructed of high deformability materials	Rigid	-	2
Motor control centres, panel boards, switch gear, instrumentation cabinets, and other components constructed of sheet metal framing	Flexible	2.5	2 - 3
Communication equipment, computers, instrumentation, and controls	Rigid	-	2 - 3
Roof-mounted stacks, cooling and electrical towers laterally braced below their centre of mass	Flexible	1.5	-
Roof-mounted stacks, cooling and electrical towers laterally braced above their centre of mass	Rigid	-	-
Other mechanical or electrical components	Rigid	-	-
Manufacturing or process conveyors (non-personnel)	Flexible	1.5	-
Vibration-isolated components and systems			
Components and systems isolated using neoprene elements and neoprene isolated floors with built-in or separate elastomeric snubbing devices or resilient perimeter stops	Flexible	1.5	-
Spring-isolated components or internally isolated components and systems and vibration-isolated floors closely restrained using built-in or separate elastomeric snubbing devices or resilient perimeter stops	Flexible	1.5	-
Suspended vibration-isolated equipment, including in-line duct devices and suspended internally isolated components	Flexible	1.5	-
Equipment support structures and platforms			
Support structures and platforms where Tp/T1 < 0.2, or Tp <= 0.05 s	Rigid	-	-
Seismic force-resisting systems with R > 3	Flexible	2.5	-
Seismic force-resisting systems with R <= 3	Flexible	1.5	-
Other systems	Flexible	1.25	-
Distribution system supports			
Tension-only and cable bracing	Rigid	-	-
Cold-formed steel rigid bracing	Rigid	-	-

Description of part or component	Inferred Class from ASCE 7-22	Expected ductility at ULS	
		ASCE 7-22	NZS 1170.5
Hot-rolled steel bracing	Rigid	-	-
Other rigid bracing	Rigid	-	-
Lateral resistance provided by rods in flexure	Flexible	1.5	
Vertical cantilever supports such as pipe tees and moment frames above and supported by a floor or roof	Flexible	1.5	
Distribution systems			
Piping, including in-line components with joints made by welding or brazing	Rigid	-	2
Piping in accordance with ASME B31, including in-line components, constructed of high- or limited deformability materials, with joints made by threading, bonding, compression couplings, or grooved couplings	Rigid	-	-
Piping and tubing not in accordance with ASME B31, including in-line components, constructed of high deformability materials, with joints made by welding or brazing	Rigid	-	-
Piping and tubing not in accordance with ASME B31, including in-line components, constructed of high or limited-deformability materials, with joints made by threading, bonding, compression couplings, or grooved couplings	Flexible	1.5	-
Piping and tubing constructed of low-deformability materials, such as cast iron, glass, and non-ductile plastics	Flexible	1.5	-
Duct systems, including in-line components, constructed of high-deformability materials, with joints made by welding or brazing	Flexible	4	3
Duct systems, including in-line components, constructed of high- or limited-deformability materials, with joints made by means other than welding or brazing 1	Flexible	4	3
Duct systems, including in-line components, constructed of low-deformability materials, such as cast iron, glass, and non-ductile plastics	Flexible	1.5	-
Electrical conduit, cable trays, and raceways	Rigid	-	3
Bus ducts or Plumbing	Rigid	-	-
Pneumatic tube transport systems	Rigid	-	-
Lighting fixtures			
Recessed	Rigid	-	1.25
Surface mounted	Rigid	-	1.25
Integrated ceiling	Rigid	-	1.25
Pendant	Flexible	-	TBDD
Personnel transportation systems			
Lift car and guide rails,	Rigid	-	2
Escalator, Lift plant	Rigid	-	3